Symmetry-adapted perturbation with half-projection for spin unrestricted geminals

Zs. É. Mihálka,[†,‡] P. R. Surján,[†] and Á. Szabados[*,†]

†*ELTE Eötvös Loránd University, Budapest, Hungary*

Faculty of Science, Institute of Chemistry

Laboratory of Theoretical Chemistry

‡ *Hevesy György PhD School of Chemistry, ELTE*

E-mail: szabados@caesar.elte.hu

Abstract

Perturbative correction to a wavefunction built from singlet-triplet mixed two-electron functions (geminals) is derived in the context of symmetry adapted schemes applying partial spin-projection. Imposing the constraint of strong orthogonality of geminals results in a reference function that captures static correlation in a computationally feasible way. In lack of spin purification, the product of spin-unrestricted geminals is spin contaminated in general, potentially undermining performance of a subsequent dynamic correlation treatment.

In this work, spin symmetry of the reference is partially restored by half-projection in a variation-after-projection scheme. Applying perturbation theory (PT) to recover the missing part of electron correlation is hampered by the fact that an obvious choice for a zero-order Hamiltonian is not provided. The situation is amended by adopting the formalism of symmetry adapted PT. The resulting framework is tested on singlet-triplet gaps of biradicaloids, and is found to perform well in situations where its unprojected counterpart fails due to spin contamination.

1 Introduction

Approximate methods aiming for accurate description of electronic structure of molecular systems having multireference character rely on a delicate balance of static and dynamic correlation. Efficient schemes for capturing the static part of electron correlation represent a crucial factor. The widely adopted complete active space (CAS)[1] method has recently reached new horizons in system size tractable, thanks to parallel computation,[2] renormalization group based techniques[3] and stochastic algorithms.[4] Formal exponential scaling of the computational cost of CAS however necessarily brings possible applications to an earlier halt than approaches having polynomial step count by construction.

Spin symmetry breaking as an economical means of incorporating static correlation was pioneered by Čížek and Paldus,[5] and followed by Yamaguchi,[6] Jordan and Silbey,[7] Pulay and co-authors.[8,9] The field has seen a recent resurgence thanks to Scuseria and co-workers, considering spatial, number and complex conjugation symmetry breaking in addition to spin symmetry at the level of a single determinant.[10,11] Spin symmetry breaking has been also investigated in connection with the general matrix product state construction.[12] The conceptual dilemma brought forth by symmetry breaking in general was termed the "symmetry dilemma" by Löwdin,[13] contemplating whether symmetry breaking and the associated variational flexibility is preferable over proper symmetry and comparatively less variational flexibility in case of an approximate wavefunction. The downside of symmetry violation was in fact observed in dynamic correlation treatments built upon a severely spin contaminated reference. Unrestricted Hartree–Fock (UHF) based Møller–Plesset (MP) methodology (UMP) is a famous example.[14–17]

Spin purification advocated by Löwdin[18,19] represents an obvious workaround that can be performed either in a projection-after-variation (PAV) or in a variation-after-projection (VAP) scenario. An unfavourable feature of the former is the emergence of non-differentiable, or even discontinuous potential curves. Size inconsistency is another unwanted consequence of spin projection. This has been reported to be of substantial magnitude within VAP

schemes starting from a different orbitals for different spin (DODS) determinant[20–22] or a geminal based wavefunction Ansatz.[23,24] When applying full spin-projection, the former treatment results in the extended Hartree–Fock (EHF) wavefunction, studied intensely in the second half of the 1900's.[25]

Performing full spin-projection along the lines suggested by Löwdin[18] is particularly tedious due to the exponential number of terms generated by the projection operator. Recent progress by Scuseria and co-workers,[11,20,26] and also by Pons Viver[27] made efficient implementation of projected schemes possible. Partial spin projection is an appealing alternative to full projection, offering the promise of less conceptual complexity as well as reduced size-inconsistency as compared with full projection. Work along this line includes that of Amos and Hall,[28,29] Schlegel,[30,31] Baker,[32,33] Yamaguchi[34,35] and many others.[36–39] Half-projection (HP) advocated by Smeyers[36] is a particularly simple partial projection scheme, that was later investigated in detail.[40–51] Half-projection retains just two of the exponential number of terms generated by Löwdin's spin-projection and eliminates[36,52] all spin contaminants of spin quantum numbers opposite to that of the target state, S. Since the largest contaminant is often the next, opposite parity S term compared with the target S, purification achieved by half-projection is considerable.[46,47,53,54]

Spin symmetry breaking introduced at the DODS level results in the UHF wavefunction, exhibiting an inherent pairing structure[28] characteristic to the strongly orthogonal geminal construction.[55,56] Allowing for full variational flexibility within this Ansatz leads to the Generalized Valence Bond Perfect Pairing (GVB-PP)[57] wavefunction when adopting the spin-singlet symmetry restriction. Symmetry breaking within the strongly orthogonal geminal concept leads to the wavefunction models termed Unrestriction in Active Pairs (UAP),[58] Unrestricted Perfect Pairing (UPP),[59] Unrestricted Singlet-type Strongly orthogonal Geminals (USSG),[60] Restricted-Unrestricted Singlet-type Strongly orthogonal Geminals (RUSSG).[61] A common feature of such geminal based approaches is that they are mostly able to catch a significant amount of static correlation. Dynamic correlation is severely underestimated,

due to the lack of intergeminal correlation. The effect of the strong orthogonality constraint was found minor in this respect.[62]

Recovering dynamic correlation, based on a reference exhibiting a geminal structure has been an active field of research. Studies starting from a singlet restricted reference are more abundant, including perturbative (PT)[62–66] and coupled-cluster (CC) methodologies[67–71] as well as reduced density matrix based approximations.[72,73] Dynamical correlation treatments starting from a spin contaminated geminal reference have been also explored.[62] We mention in particular MP methodology based upon the UHF wavefunction[14–17] as well as our recent studies starting from the spin-unrestricted strongly orthogonal geminal Ansatz.[74]

This latter work called the attention to the fact that spin contamination of the reference can severely undermine the performance of PT not only in a single reference framework but also at the multireference level. Since full spin projection of the spin-unrestricted geminal model was found considerably affected by size-inconsistency,[23] a midway solution has been recently explored in the form of half-projection.[24] The resulting Ansatz, termed half-projected strictly localized geminals (HP-SLG) was found to have desirable properties: reduced spin contamination as well as suppressed size inconsistency. However, HP-SLG is still missing most of the dynamic effects. In the present work we aim at developing a perturbative correction to the partially spin purified geminal-based reference, HP-SLG.

Perturbative treatment of a symmetry adapted reference has been subject to extensive research in connection with intermolecular interactions. With the product wavefunction of separated systems taken as starting point, RSPT yields poor results.[75] Restoring antisymmetry between weakly interacting fragments was found essential for obtaining reliable PT corrections. Symmetry adapted PT (SAPT) was developed to handle this problem, pioneered by Hirschfelder,[76–78] Van der Avoird,[79,80] Murrell and Shaw[81] as well as Claverie,[82] and later Jeziorski, and co-workers,[83–86] to name a few. A comparative study on several different formalisms of SAPT was presented by Jeziorski *et al.*[86] The PT frameworks applied in the present study are essentially adaptations of SAPT with HP playing the role of symmetry

projection. We apply the so-called weak symmetry forcing SAPT variant, with occasional tests shown for strong symmetry forcing or an approximate version thereof.

The paper is organized as follows. Half-projected geminal product Ansatz and the symmetry projected PT formulae relevant in our case are presented shortly in Sec. 2.1 and 2.2. This settles the context of the work. Main achievement of this study, presented in Sec. 2.3, constitutes the details of adopting SAPT for the half-projection operator and the SLG reference. Designing a well performing theoretical setup is in fact far from being straightforward in these circumstances, and consumed most effort spent in this work. Details of numerical computations and illustrative applications, focusing on singlet-triplet splittings are given in Sec. 3 and Sec. 4, respectively.

2 Theory

2.1 Half-projected Geminal product Ansatz

In what follows, we are only concerned with states which are eigenstates of operator $\hat{S}_z$ with eigenvalue $M_S = 0$. The building blocks of the model are two-electron functions (geminals) expressed as

$$\psi_\mu^+ = \sum_{ij}^{(\mu)} C_{ij}\, i_\beta^+ j_\alpha^+ \ , \tag{1}$$

where Greek indices label geminals, while Latin indices $i, j, k, \ldots$ refer to spatial orbitals. Strong orthogonality of geminals[55,56] is ensured by different geminals being expanded over pairwise disjoint sets of spatial orbitals (cf. summation notation in Eq.(1)), meaning that each orbital is assigned to at most one geminal. Orbitals corresponding to the same two-electron block generate a so-called geminal subspace. The strictly localized geminals (SLG) Ansatz[87–89] is defined as

$$|\mathrm{SLG}\rangle = \prod_{\mu}^{N/2} \psi_\mu^+ \, |\mathrm{vac}\rangle \ , \tag{2}$$

where N denotes the even number of electrons in the system.

Geminal coefficient matrix $\boldsymbol{C}$ formed of elements C_{ij} of Eq.(1) has no apparent symmetry for SLG. Its block diagonal nature is a consequence of strong orthogonality, its block corresponding to geminal μ is denoted by $\boldsymbol{C}_\mu$. Block $\boldsymbol{C}_\mu$ can be decomposed into a symmetric and a skew-symmetric matrix, ${}^{\mathrm{s}}\boldsymbol{C}_\mu$ and ${}^{\mathrm{a}}\boldsymbol{C}_\mu$, respectively. Without loss of generality, we assume that ${}^{\mathrm{s}}\boldsymbol{C}_\mu$ is diagonal for all geminals. Symmetric part of $\boldsymbol{C}_\mu$ generates the singlet component of geminal ψ_μ, while ${}^{\mathrm{a}}\boldsymbol{C}_\mu$ corresponds to the triplet part. Orbitals diagonalizing the singlet part of $\boldsymbol{C}$ will be called "singlet natural" orbitals.

Geminals are assumed to be normalized:

$$\sum_{ij}^{(\mu)} |C_{ij}|^2 = 1 \ , \tag{3}$$

from which $\langle \mathrm{SLG}|\mathrm{SLG}\rangle = 1$ follows. A two-dimensional, normalized spin-mixed geminal can be described by two configuration interaction (CI) parameters in its singlet natural form, according to

$$\boldsymbol{C}_\mu = \begin{pmatrix} \cos(\delta_\mu)\cos(\eta_\mu) & \sin(\delta_\mu)/\sqrt{2} \\ -\sin(\delta_\mu)/\sqrt{2} & -\cos(\delta_\mu)\sin(\eta_\mu) \end{pmatrix} \ . \tag{4}$$

Parameter δ_μ tunes the relative weight of the singlet and triplet components, while parameter η_μ is responsible for correlation in the singlet part.

Several wavefunctions represent a special case of the SLG family, UHF[90] and GVB–PP[57] are the most widely known among these. Antisymmetrized Product of Strongly Orthogonal Geminals (APSG),[56,91–93] UAP[58] and RUSSG[61] also belong to this category. A comparative account on these models is given e.g. in Ref.[23]

The SLG wavefunction of Eq.(2) is in general spin-contaminated, which is remedied partly by applying half-projection[36] defined as

$$\hat{P}_S = \frac{1}{2}\left(1 \ + \ f\hat{\mathcal{P}}_{\mathrm{sf}}\right) \ , \tag{5}$$

where $f = (-1)^S$ with S standing for the desired overall spin quantum number. Operator

$\hat{\mathcal{P}}_{\rm sf}$ is the spin-flip operator, its effect on an $M_S = 0$ determinant is evaluated as

$$\begin{aligned} \hat{\mathcal{P}}_{\rm sf}\, i^+_\beta \ldots j^+_\beta k^+_\alpha \ldots l^+_\alpha |{\rm vac}\rangle &= k^+_\beta \ldots l^+_\beta i^+_\alpha \ldots j^+_\alpha |{\rm vac}\rangle \\ &= (-1)^{N/2} i^+_\alpha \ldots j^+_\alpha k^+_\beta \ldots l^+_\beta |{\rm vac}\rangle \ , \end{aligned} \tag{6}$$

where $N/2 = n_\alpha = n_\beta$.

The half-projected SLG function takes the form

$$|\text{HP-SLG}\rangle = \hat{P}_S |\text{SLG}\rangle \ . \tag{7}$$

Note, that since $\hat{P}_S$ does not eliminate all contaminants, weight of *all* remaining components is increased in HP-SLG as compared with SLG (not only that of the target component). The HP-SLG function, derived according to Eq.(7) from the normalized SLG function is not normalized in general. Its squared norm can be expressed as

$$\langle \text{HP-SLG} \,|\, \text{HP-SLG}\rangle = \frac{1 \ + \ f\mathcal{M}}{2} \ , \tag{8}$$

with

$$\begin{aligned} \mathcal{M} &= \prod_{\mu}^{N/2} \mathcal{M}_\mu \\ \mathcal{M}_\mu &= \sum_{i}^{(\mu)} \left(C^T C^*\right)_{ii} = \sum_{ij}^{(\mu)} C_{ij} C^*_{ji} \ , \end{aligned} \tag{9}$$

The HP-SLG model is obtained by setting the HP-SLG energy

$$E_{\rm HP} = \frac{\langle \text{HP-SLG} \,|\, \hat{H} \,|\, \text{HP-SLG}\rangle}{\langle \text{HP-SLG} \,|\, \text{HP-SLG}\rangle} \ . \tag{10}$$

stationary with respect to geminal coefficients, i.e., within a VAP scheme. In principle, HP-SLG can be also set stationary with respect to unitary transformation of orbitals, but it is not carried out in this work.

The condition of geminal coefficients being optimal can be recast as separate pseudo eigenvalue equations for each geminal

$$\hat{H}_\mu^{\rm eff}\ \psi_\mu = E_\mu\ \psi_\mu\ , \quad \mu = 1, \ldots, N/2 \tag{11}$$

with the effective geminal Hamiltonian, $\hat{H}_\mu^{\rm eff}$ reading as

$$\hat{H}_\mu^{\rm eff} = {}^{\mathcal{N}}\hat{H}_\mu\ +\ f\ {}^{\mathcal{M}}\hat{H}_\mu\,\hat{\mathcal{P}}_{\mu,\rm sf}\ -\ f\,L_\mu\,\hat{\mathcal{P}}_{\mu,\rm sf}\ , \tag{12}$$

where

$$ {}^{\mathcal{N}}\hat{H}_\mu = \sum_{kl}^{(\mu)}\left({}^{\mathcal{N}}F_{kl}^a k_\alpha^+ l_\alpha^-\ +\ {}^{\mathcal{N}}F_{kl}^b k_\beta^+ l_\beta^-\right) + \frac{1}{2}\sum_{klmn}^{(\mu)}[kl|mn]\sum_{\sigma,\sigma'} k_\sigma^+ l_{\sigma'}^+ n_{\sigma'}^- m_\sigma^- \tag{13a}$$

$$ {}^{\mathcal{M}}\hat{H}_\mu = \frac{\mathcal{M}}{\mathcal{M}_\mu}\left\{\sum_{kl}^{(\mu)}\left({}^{\mathcal{M}}F_{kl}^a k_\alpha^+ l_\alpha^-\ +\ {}^{\mathcal{M}}F_{kl}^b k_\beta^+ l_\beta^-\right) + \frac{1}{2}\sum_{klmn}^{(\mu)}[kl|mn]\sum_{\sigma,\sigma'} k_\sigma^+ l_{\sigma'}^+ n_{\sigma'}^- m_\sigma^-\right\} \tag{13b}$$

$$ L_\mu = \frac{\mathcal{M}}{\mathcal{M}_\mu}\left({}^{\mathcal{M}}\Lambda_\mu + \frac{\Theta}{1+f\,\mathcal{M}}\right) \tag{13c}$$

Expressions for the Fockians ${}^{\mathcal{N}}\boldsymbol{F}^a$, ${}^{\mathcal{N}}\boldsymbol{F}^b$, ${}^{\mathcal{M}}\boldsymbol{F}^a$ and ${}^{\mathcal{M}}\boldsymbol{F}^b$ as well as quantities ${}^{\mathcal{M}}\Lambda_\mu$ and Θ are given in Ref.[24] Two-electron integrals $[ij|kl]$ are written above in $[12|12]$ convention. Operator $\hat{\mathcal{P}}_{\mu,\rm sf}$ is the 'local' spin-flip corresponding to geminal μ, flipping the spin of orbitals belonging to subspace μ. Eq.(11) for $\mu = 1, \ldots, N/2$ is solved in an iterative (self-consistent) manner. Upon reaching a converged solution, *all* $M_S = 0$ two-electron eigenstates of operator $\hat{H}_\mu^{\rm eff}$ are obtained, labeled as $\psi_{\mu,j}$, $(j = 0, 1, \ldots)$, with corresponding eigenvalues $E_{\mu,j}$, where $\psi_{\mu,0}$ denotes the geminal entering the HP-SLG Ansatz (cf. Eqs.(7) and (2)). Appearance of $\hat{\mathcal{P}}_{\mu,\rm sf}$ makes a marked difference in the effective Hamiltonians of Eq.(12) and that of Eq.(11) in Ref.,[24] as the latter does not contain $\hat{\mathcal{P}}_{\mu,\rm sf}$ explicitly. Instead, the effect of the local spin-flip is absorbed in the second-quantized form of $\hat{H}_\mu^{\rm eff}$, with the assumption that $M_S = 0$ two-electron functions constructed with orbitals of subspace μ represent its domain. While action of the two Hamiltonians is the same on this subspace, their effect is different in other

subspaces of the Hilbert space. In the present work besides geminal states $\psi_{\mu,j}$, $M_S \neq 0$ two-electron functions as well as one-, three- and four-electron fragments appear in subspace μ in course of the PT treatment. This is the reason for indicating the local spin-flip explicitly in Eq.(12).

2.2 Half-projected Geminal-based PT

Perturbation theory based on geminal product wavefunctions falls into the multireference category. Geminal construction offers a plausible way of defining a zero-order Hamiltonian for the PT treatment in the form

$$\hat{H}^{(0)} = \sum_{\mu=1}^{N/2} \hat{H}_\mu \ + \ \hat{H}_V^{(0)} \ . \tag{14}$$

In the above, $\hat{H}_\mu$ is an effective Hamiltonian acting on subspace μ and including other orbitals in an implicit manner. Effective Hamiltonians in Eq.(14) are similar in spirit to that of Eq.(12), but their actual form is different, as discussed later. $V = N/2 + 1$ labels the virtual subspace in Eq.(14), collecting orbitals not assigned to any two-electron fragment. As a consequence of Eq.(11) the zero order equation is fulfilled for the geminal product

$$\hat{H}^{(0)}|\mathrm{SLG}\rangle = \left(\sum_{\mu=1}^{N/2} E_\mu \right) |\mathrm{SLG}\rangle = E^{(0)}|\mathrm{SLG}\rangle \tag{15}$$

i.e., $|\Psi^{(0)}\rangle = |\mathrm{SLG}\rangle$. Excited functions $|\Psi_K^{(0)}\rangle$ ($K \neq 0$), orthogonal to $|\mathrm{SLG}\rangle$, used for expanding the first order PT correction $|\Psi^{(1)}\rangle$ as

$$|\Psi^{(1)}\rangle = \sum_{K\neq 0} c_K^{(1)} |\Psi_K^{(0)}\rangle \tag{16}$$

are conveniently obtained in the product form akin to $|\mathrm{SLG}\rangle$, with the general form

$$|\Psi_K^{(0)}\rangle = \prod_\mu \varphi^+_{\mu,K}|\mathrm{vac}\rangle \ , \tag{17}$$

where fragments $\varphi_{\mu,K}$ constituting $|\Psi_K^{(0)}\rangle$, constructed within separate geminal subspaces, can be furnished with $1,\ldots,4$ electrons. Following the notation of Ref.,[74] excited states are categorized according to the number of geminals differing from those constituting $|\mathrm{SLG}\rangle$. Within categories, excitation cases are defined based on the number of alpha and beta electrons occupying the excited fragments. States $|\Psi_K^{(0)}\rangle$ are not necessarily eigenstates of $\hat{H}^{(0)}$, implying a nondiagonal $\boldsymbol{G}$ used for determining coefficients $c_K^{(1)}$ from the first order equation

$$\sum_{K\neq 0} G_{LK}\ c_K^{(1)} = -\,H_{L0}\ , \qquad \forall\, L\neq 0\ , \tag{18}$$

where $G_{LK} = \langle\Psi_L^{(0)}|\hat{H}^{(0)}|\Psi_K^{(0)}\rangle - E^{(0)}\delta_{LK}$ and $H_{L0} = \langle\Psi_L^{(0)}|\hat{H}|\mathrm{SLG}\rangle$. The advantage of the choice of Eq.(14) is that $\boldsymbol{G}$ exhibits a block-diagonal character, facilitating an efficient solution[64,74,94] of the system of linear equations of Eq.(18). Different cases of excitations within excited state categories form the individual blocks of $\boldsymbol{G}$.

The above approach was advocated by Kapuy in the 60s[95,96] and has been exploited in PT schemes designed in our laboratory based on spin-restricted,[56] as well as unrestricted[74] geminal product zero-order. A Block Correlated PT2 scheme with GVB–PP as reference (GVB-BCPT2) involving a diagonal zero-order operator and treating virtual orbitals individually was also explored.[94] These studies can be considered as forerunners of the present work which aims at correcting the half-projected counterpart of $|\mathrm{SLG}\rangle$. Since the symmetry projected geminal function does not arise as eigenvector of a sum of effective geminal Hamiltonians a decision is to be made at this point. One may stick to the half-projected function as $|\Psi^{(0)}\rangle$ and tailor a zero-order Hamiltonian to obtain an appropriate zero-order equation. This route was taken e.g. by Tsuchimochi and Ten-no[97] when correcting the EHF function by PT.

Another grab on the problem is provided by sticking with the zero-order equation of Eq.(15) and incorporating symmetry projection in the PT treatment. Starting from the EHF function, this option has been also explored, cf. the work by Tsuchimochi and Van Voorhis.[98] Knowles and Handy also applied this method for correcting the PAV-type projected UHF reference by PT.[99] The framework of SAPT, studied extensively in connection with weak intermolecular interactions follows this latter route. It was pointed out,[100] that there is no unique projected PT scheme. In fact, the above mentioned works on correcting symmetry breaking HF reference functions can be regarded as adaptations of particular SAPT variants. The same holds for the approach followed in this work in designing a PT correction. A concise presentation of the relevant formulae is given below for completeness.

Suppose we have a symmetry operator $\hat{\mathcal{A}}$, fulfilling $[\hat{H}, \hat{\mathcal{A}}] = 0$. If $\hat{P}$ projects onto a subspace spanned by the the eigenvectors of $\hat{\mathcal{A}}$ corresponding to some of its eigenvalues, it follows that $[\hat{H}, \hat{P}] = 0$. Our aim now is to derive PT corrections to an initial wavefunction for which $\hat{P}|\Psi^{(0)}\rangle \neq |\Psi^{(0)}\rangle$.

Start from the Schrödinger equation written for the exact solution $|\Psi\rangle$, multiplied by $\hat{P}$

$$\hat{H}\hat{P}|\Psi\rangle = E\hat{P}|\Psi\rangle \ . \tag{19}$$

Upon introducing the partitioning $\hat{H} = \hat{H}^{(0)} + \hat{W}$ fulfilling

$$\hat{H}^{(0)}|\Psi^{(0)}\rangle = E^{(0)}|\Psi^{(0)}\rangle \tag{20}$$

one may arrive at the projected nth order equation in the general form

$$\langle\phi|\hat{H}^{(0)}\hat{P}\Psi^{(n)}\rangle + \langle\phi|\hat{W}\hat{P}\Psi^{(n-1)}\rangle = \sum_{k=0}^{n} \mathcal{E}^{(k)}\langle\phi|\hat{P}\Psi^{(n-k)}\rangle \tag{21}$$

where $\Psi^{(n)}$ is the n-th term of the Taylor series of Ψ, $\langle\phi|$ is a state up to our choice and $\mathcal{E}^{(n)}$ matches the n-th term of the Taylor series of E when $[\hat{H}^{(0)}, \hat{P}] = 0$. While $\sum_n \mathcal{E}^{(n)}$ agrees

with the exact energy upon convergence of the series, individual terms differ from the partial sums of the Taylor series of E when $\hat{H}^{(0)}$ does not commute with $\hat{P}$.

As the corrections $\hat{P}|\Psi^{(n)}\rangle$ are in general linearly dependent (overcomplete),[101] $\mathcal{E}^{(n)}$ is not well-defined. Multiple definitions (and values) may be given depending on the choice for $\langle\phi|$ in Eq.(21), two plausible ideas being $\langle\phi| = \langle\Psi^{(0)}|$ and $\langle\phi| = \langle\Psi^{(0)}|\hat{P}$. The latter requires computation of terms $\langle\Psi^{(0)}|\hat{P}\hat{H}^{(0)}\hat{P}\Psi^{(n)}\rangle$ and $\langle\Psi^{(0)}|\hat{P}\hat{W}\hat{P}\Psi^{(n-1)}\rangle$, which usually makes evaluation more complicated. Hence we stick to the former choice.

Setting $|\phi\rangle = |\Psi^{(0)}\rangle$, one arrives at[99]

$$\begin{aligned}\mathcal{E}^{(0)} =& E^{(0)}\\ \mathcal{E}^{(0)} + \mathcal{E}^{(1)} =& \langle\Psi^{(0)}|\hat{H}\hat{P}|\Psi^{(0)}\rangle \;/\; \langle\Psi^{(0)}|\hat{P}|\Psi^{(0)}\rangle = E_{\mathrm{HP}}\end{aligned}$$

and

$$\mathcal{E}^{(2)} = \langle\Psi^{(0)}|(\hat{H} - E_{\mathrm{HP}})\hat{P}|\Psi^{(1)}\rangle \;/\; \langle\Psi^{(0)}|\hat{P}|\Psi^{(0)}\rangle \tag{22}$$

with $\Psi^{(1)}$ obtained from Eqs.(16)-(18). Eq.(22) matches the SAPT energy expression obtained by so-called weak symmetry forcing.[84,86]

In our case the general formula of Eq.(22) is to be applied with the projection operator performing HP according to Eq.(5). With $|\mathrm{SLG}\rangle$ substituted for $|\Psi^{(0)}\rangle$, Eq.(22) takes the form

$$\mathcal{E}^{(2)} = \frac{\langle\mathrm{SLG}|\hat{H}|\Psi^{(1)}\rangle + f\,\langle\mathrm{SLG}|\hat{\mathcal{P}}_{\mathrm{sf}}\hat{H}|\Psi^{(1)}\rangle - f\,E_{\mathrm{HP}}\langle\mathrm{SLG}|\hat{\mathcal{P}}_{\mathrm{sf}}\Psi^{(1)}\rangle}{1 + f\,\mathcal{M}}\ , \tag{23}$$

where relation $[\hat{H}, \hat{\mathcal{P}}_{\mathrm{sf}}] = 0$ was taken advantage of, and $\mathcal{M}$ is given by Eq.(9). Introducing first order coefficients arising from Eq.(18) provides the shorter expression

$$\mathcal{E}^{(2)} = \frac{\sum_{K\neq 0} c_K^{(1)}(H_{0K} + f\,\widetilde{H}_{0K} - f\,E_{\mathrm{HP}}M_{0K})}{1 + f\,\mathcal{M}}\ , \tag{24}$$

where $\widetilde{H}_{0K} = \langle\mathrm{SLG}|\hat{H}\hat{\mathcal{P}}_{\mathrm{sf}}|\Psi_K^{(0)}\rangle$, $M_{0K} = \langle\mathrm{SLG}|\hat{\mathcal{P}}_{\mathrm{sf}}\Psi_K^{(0)}\rangle$.

When adopting strong symmetry forcing[78–80] according to SAPT terminology, a different

second-order energy formula is obtained, reading as

$$\begin{aligned}\mathcal{E}_{\mathrm{s}}^{(2)} &= -\frac{\langle \mathrm{SLG}|(\hat{H}-E_{\mathrm{HP}})\hat{P}_S\hat{Q}\hat{P}_S(\hat{H}-E_{\mathrm{HP}})|\mathrm{SLG}\rangle}{\langle SLG|\hat{P}_S|\mathrm{SLG}\rangle} \\ &= \mathcal{E}^{(2)} + \frac{\langle \mathrm{SLG}|\hat{H}\hat{Q}\hat{H}|\mathrm{SLG}\rangle - \langle \mathrm{SLG}|\hat{\mathcal{P}}_{\mathrm{sf}}(\hat{H}-E_{\mathrm{HP}})\hat{Q}(\hat{H}-E_{\mathrm{HP}})\hat{\mathcal{P}}_{\mathrm{sf}}|\mathrm{SLG}\rangle}{2(1+f\ \mathcal{M})}\ ,\end{aligned} \tag{25}$$

where $\hat{Q}$ stands for the reduced resolvent, i.e., the inverse of $(\hat{H}^{(0)} - E^{(0)})$ in the space orthogonal to $|\mathrm{SLG}\rangle$ (thus its matrix representation corresponds to the inverse of $\boldsymbol{G}$). The last term in Eq.(25) necessitates the inclusion of higher excitations than those contributing to $\mathcal{E}^{(2)}$, due to the appearance of the term featuring two instances of $\hat{\mathcal{P}}_{\mathrm{sf}}$. Rewriting this term as

$$\langle \mathrm{SLG}|\hat{\mathcal{P}}_{\mathrm{sf}}(\hat{H}-E_{\mathrm{HP}})\hat{Q}(\hat{H}-E_{\mathrm{HP}})\hat{\mathcal{P}}_{\mathrm{sf}}|\mathrm{SLG}\rangle = \sum_{K,L\neq 0}(\widetilde{H}_{0K} - E_{\mathrm{HP}}\,M_{0K})Q_{KL}(\widetilde{H}_{L0} - E_{\mathrm{HP}}M_{L0}) \tag{26}$$

makes it apparent that excited states $|\Psi_K^{(0)}\rangle$ contributing to the second order energy in this scheme are those for which $\widetilde{H}_{0K}$ is nonzero: elements of the first order interacting space of $|\mathrm{SLG}\rangle$, or any excited state that can be obtained from those states via excitations that are M_S and electron number preserving geminal-wise. Appearance of higher-order excitations highlights the difference between weak and strong symmetry forcing: in the latter, a symmetry projector is inserted into more than one position in the PT formulae, resulting in a computationally more demanding expression.

2.3 Particulars of HP-SLG PT

2.3.1 Definition of $\hat{H}^{(0)}$

Performance of PT strongly depends on the choice for the zero-order Hamiltonian. The PT scheme described in Sec. 2.2 necessitates a $\hat{H}^{(0)}$ fulfilling Eq.(20), with the unprojected geminal product as eigenfunction. The sum of effective operators, Eq.(14) serves for this

purpose having the advantage that $\hat{H}_\mu$ incorporates intrageminal two-electron terms and that a decoupling of the equations yielding $|\Psi^{(1)}\rangle$ is provided due to the block-diagonal structure of $\boldsymbol{G}$, cf. Eq.(18). The eigenvalue equation of the effective Hamiltonian, Eq.(11) in principle ensures the zero order equation when writing Eq.(14) with $\hat{H}_\mu^{\text{eff}}$ of Eq.(12). Note, that $\psi_{\mu,j}$ in general differ for variationally optimized SLG and HP-SLG in accordance with H_μ^{eff} being different for the two schemes.

While the effective Hamiltonian of Eq.(12) is suitable from the part of the geminal solution $\psi_{\mu,0}$, the same does not necessarily apply for other geminal states. Concerns arise with spin-flip involving terms of Eq.(12) (second and third terms on the right hand side), which stem from purifying the *geminal product* involving $\psi_{\mu,0}$, with factor f defined for the target spin of the many-electron state. This calls for caution when considering excited geminal states, the spin of which are not related to that of the HP-SLG function. Further precaution is warranted when evaluating the effect of the local spin-flip on $M_S \neq 0$ states. Since geminal functions contributing to SLG are all characterized by $M_S = 0$, this situation does not show up in the context of HP-SLG, but it must be considered when $\hat{\mathcal{P}}_{\mu,\text{sf}}$ involving terms are admitted in $\hat{H}^{(0)}$ with the purpose of developing PT. A straightforward generalization of $\hat{\mathcal{P}}_{\mu,\text{sf}}$ for $M_S \neq 0$ states results in undesirable $\hat{S}_z$-violation at the level of $\hat{H}_\mu$ and consequently by $\hat{H}^{(0)}$. When applying $\hat{\mathcal{P}}_{\mu,\text{sf}}$ in this work, a workaround suggested by Ruiz[102] is adopted to conserve M_S. We refer to Appendix A for further details on this.

A desirable feature of effective Hamiltonians in the half-projected framework is that they should fall back to their spin-pure counterparts if the reference is spin-pure. In general, if each geminal is an eigenstate of $\hat{S}^2$ (i.e., either purely singlet or purely triplet), operator $\hat{H}_\mu$ of Eq.(12) simplifies to

$$ {}^{\mathcal{N}}\hat{H}_\mu(1 + f\,\frac{\mathcal{M}}{\mathcal{M}_\mu}\,\hat{\mathcal{P}}_{\mu,\text{sf}}) - f\,\frac{\mathcal{M}}{\mathcal{M}_\mu}\,E_{\mu,0}\,\hat{\mathcal{P}}_{\mu,\text{sf}}\ , \tag{27} $$

and ${}^{\mathcal{N}}\hat{H}_\mu$ is spin-pure in such a case. Though eigenstates of Eq.(27) are the same as those

of ${}^{\mathcal{N}}\hat{H}_\mu$ in the $M_S = 0$ subspace, energy levels are different with the exception of $E_{\mu,0}$ corresponding to $\psi_{\mu,0}$. It is at this point where the caveat to plugging the full form of Eq.(12) in Eq.(14) can be argued. When all geminals are singlet, the energy of an excited singlet state $\psi_{\mu,j}, j \neq 0$ (cf. excited solutions of Eq.(11)) of geminal μ by Eq.(27) is given as $2E_{\mu,j} - E_{\mu,0}$ instead of the desired $E_{\mu,j}$. The case of the $M_S = 0$ triplet state is even more pathological, it appearing as a downright intruder at the level of two-electron fragments, with eigenvalue $E_{\mu,0}$. The effect of the effective operator in Eq.(27) on spin-pure geminal states is worked out in detail in Sec. A.2 of Appendix A. It is also discussed there that the noninteracting nature of singlets with triplets cannot be called upon to alleviate the problem. The ill-effect can be clearly attributed to the second and third terms on the right hand side of Eq.(12), which are however needed for ensuring Eq.(20).

To remedy the situation, distinct effective Hamiltonians are formulated in distinct subspaces of functions corresponding to geminal index μ. The three subspaces introduced are associated with projectors

$$\begin{aligned} \hat{O}_\mu &= |\psi_{\mu,0}\rangle\langle\psi_{\mu,0}| \\ \hat{R}_\mu &= \sum_{j\neq 0} |\psi_{\mu,j}\rangle\langle\psi_{\mu,j}| \\ \hat{Q}_\mu &= 1 - \hat{O}_\mu - \hat{R}_\mu \ , \end{aligned} \tag{28}$$

where states $\psi_{\mu,j}$ $(j = 0, 1, \ldots)$ are the $M_S = 0$ solutions of Eq.(11), defined under Eq.(13), while projector $\hat{Q}_\mu$ involves $M_S \neq 0$ two-electron states in subspace μ as well as one-, three- and four-electron states. With the use of projectors $\hat{O}_\mu$, $\hat{R}_\mu$ and $\hat{Q}_\mu$, the effective Hamiltonian entering Eq.(14) is defined for $\mu \leq N/2$ as

$$\hat{H}_\mu = E_{\mu,0}\,\hat{O}_\mu + \hat{R}_\mu\,\hat{H}^R_\mu\,\hat{R}_\mu + \hat{Q}_\mu\,\hat{H}^Q_\mu\,\hat{Q}_\mu \ . \tag{29}$$

Of the several choices for quantities $\hat{H}^R_\mu$ and $\hat{H}^Q_\mu$, three are reported in Section 4. Partitioning variants are formulated with the aim of avoiding intruder effects as well as fine-tuning performance. The cure e.g. for the above mentioned intruder problem, affecting space R_μ,

is prompted by the following rewriting of Eq.(11)

$$\left({}^{\mathcal{N}}\hat{H}_\mu \;+\; f\;{}^{\mathcal{M}}\hat{H}_\mu\,\hat{\mathcal{P}}_{\mu,\mathrm{sf}}\right)\psi_\mu = E_\mu\psi_\mu \;+\; f\,L_\mu\,\hat{\mathcal{P}}_{\mu,\mathrm{sf}}\,\psi_\mu\;. \tag{30}$$

We now proceed by substituting $\mathcal{M}\mathcal{M}_\mu^{-1}E_\mu$ in place of L_μ on the right hand side. Though this violates the equation above, it presents no serious concern as we merely aim at formulating a suitable $\hat{H}_\mu$ for space R_μ . Note however, that $\mathcal{M}\mathcal{M}_\mu^{-1}E_\mu$ and L_μ match in the spin-pure case, deviation from Eq.(30) can therefore be expected to be small when spin contamination is small. The substitution is motivated by the observation that $(1 + f\,\frac{\mathcal{M}}{\mathcal{M}_\mu}\hat{\mathcal{P}}_{\mu,\mathrm{sf}})$ appears on the right hand side as a sort of metric. This hints to consider

$$\left(1 + f\,\frac{\mathcal{M}}{\mathcal{M}_\mu}\hat{\mathcal{P}}_{\mu,\mathrm{sf}}\right)^{-1}\left({}^{\mathcal{N}}\hat{H}_\mu \;+\; f\;{}^{\mathcal{M}}\hat{H}_\mu\,\hat{\mathcal{P}}_{\mu,\mathrm{sf}}\right) \tag{31}$$

as effective Hamiltonian. Formally, operator $1 + f\,\frac{\mathcal{M}}{\mathcal{M}_\mu}\hat{\mathcal{P}}_{\mu,\mathrm{sf}}$ is invertible in the $M_S = 0$ two-electron subspace if and only if $\left|\frac{\mathcal{M}}{\mathcal{M}_\mu}\right| \neq 1$, which excludes the spin-pure case. In general, if some of the two-electron fragments are spin-mixed, then $\left|\frac{\mathcal{M}}{\mathcal{M}_\mu}\right|$ usually differs from 1, not causing an issue with inversion. For spin-pure cases, a workaround is provided in Appendix A. We proceed in the spirit of Eq.(31), and find treatment for the defect caused by $\hat{\mathcal{P}}_{\mu,\mathrm{sf}}$ in simply omitting it, leading to the expression

$$\hat{H}^{\mathrm{c}}_\mu \;=\; \frac{{}^{\mathcal{N}}\hat{H}_\mu \;+\; f\;{}^{\mathcal{M}}\hat{H}^s_\mu}{1 \;+\; f\,\frac{\mathcal{M}}{\mathcal{M}_\mu}}\;. \tag{32}$$

In the above ${}^{\mathcal{M}}\hat{H}^s_\mu$ stands for the hermitian part of ${}^{\mathcal{M}}\hat{H}_\mu$

$${}^{\mathcal{M}}\hat{H}^s_\mu \;=\; ({}^{\mathcal{M}}\hat{H}_\mu \;+\; {}^{\mathcal{M}}\hat{H}^\dagger_\mu)/2\;. \tag{33}$$

This amendment becomes necessary due to the fact that ${}^{\mathcal{M}}\hat{H}_\mu$ is non-Hermitian in general, as discussed in Appendix A. Geminal energies by Eq.(32) are found to agree with that of

${}^{\mathcal{N}}\hat{H}_\mu$ in the spin-pure limit for $\mathcal{M}_\mu = 1$, the intruder problem mentioned above is therefore resolved.

As an alternative approach, one may think of removing the artificial intruder in the spin-pure case for $j \neq 0$ via an additive correction by $E_{\mu,0}$ and a scaling by 1/2. In the general, spin contaminated case this takes the form of a shift by $f\mathcal{M}\mathcal{M}_\mu^{-1}E_{\mu,0}$ and a scaling by $(1 + f\mathcal{M}\mathcal{M}_\mu^{-1})^{-1}$. The corresponding modification of Eq.(12) leads to

$$\hat{H}_\mu^{\mathrm{b}} = \left({}^{\mathcal{N}}\hat{H}_\mu + f\,\left({}^{\mathcal{M}}\hat{H}_\mu\,\hat{\mathcal{P}}_{\mu,\mathrm{sf}}\right)^s - f\,L_\mu\hat{\mathcal{P}}_{\mu,\mathrm{sf}} + f\,\frac{\mathcal{M}}{\mathcal{M}_\mu}E_{\mu,0}\right) / \left(1\ +\ f\,\frac{\mathcal{M}}{\mathcal{M}_\mu}\right)\ , \tag{34}$$

and the symmetrized form of ${}^{\mathcal{M}}\hat{H}_\mu\,\hat{\mathcal{P}}_{\mu,\mathrm{sf}}$ is applied in analogy with Eq.(33). It is easy to show, that while Eq.(34) cures the problem of the artifical shift of singlet states, it leaves $M_S = 0$ triplet states degenerate with the singlet $\psi_{\mu,0}$ ground state geminal. The effective Hamiltonian $\hat{H}_\mu^{\mathrm{b}}$ is therefore not appropriate for space O_μ. Note that $\hat{H}_\mu^{\mathrm{c}}$ can be derived in this alternative route also by omitting $\hat{\mathcal{P}}_{\mu,\mathrm{sf}}$ from $\hat{H}_\mu^{\mathrm{b}}$ and dropping the last two terms of the numerator.

In the general case there is no guarantee for the denominator of Eq.(32) and Eq.(34) not becoming zero. A discussion and workaround for the spin-pure case is presented in Appendix A. In the general case the following modification may be of help:

$$\hat{H}_\mu^{\mathrm{d}}\ =\ \frac{{}^{\mathcal{N}}\hat{H}_\mu\ +\ f\ \mathcal{M}_\mu\ {}^{\mathcal{M}}\hat{H}_\mu^s}{1\ +\ f\,\mathcal{M}}\ . \tag{35}$$

Apparently $\mathcal{M}_\mu$ is introduced in the second term both in the numerator and the denominator when stepping to Eq.(35) from Eq.(32). This may be argued with the observation that $f\mathcal{M}$ is positive and effect of $\hat{\mathcal{P}}_{\mu,\mathrm{sf}}/\mathcal{M}_\mu$ is unit in space R_μ in the spin-pure case, cf. Appendix A. The sign of the second term in the round braces in Eq.(31) is therefore spoiled when omitting just $\hat{\mathcal{P}}_{\mu,\mathrm{sf}}$. In this view, Eq.(35) corresponds to omitting $\hat{\mathcal{P}}_{\mu,\mathrm{sf}}/\mathcal{M}_\mu$ from Eq.(31). One may also realize the reassuring fact, that the denominator of Eq.(35) is proportional to Eq.(8). The quantity in Eq.(8) tends to zero only in the limit of projecting an essentially spin-pure

geminal product in the wrong direction, i.e., using $f = 1$ for a triplet $|\mathrm{SLG}\rangle$ (i.e., $\mathcal{M} = -1$) or $f = -1$ for a singlet $|\mathrm{SLG}\rangle$ (i.e., $\mathcal{M} = 1$). Since this situation is clearly pathological and can be excluded by start, we consider the geminal Hamiltonian $\hat{H}^{\mathrm{d}}_{\mu}$ of Eq.(35) as one choice, suitable for our purpose.

With the aim of modifying the least possible when arriving to $\hat{H}_{\mu}$, one may envisage yet another alternative route, rewriting the geminal eigenvalue equation, Eq.(30) in the form

$$\left({}^{\mathcal{N}}\hat{H}_{\mu} \;+\; f\;{}^{\mathcal{M}}\hat{H}_{\mu}\,\hat{\mathcal{P}}_{\mu,\mathrm{sf}}\right)\psi_{\mu} = E_{\mu}\left(1 \;+\; f\,\frac{L_{\mu}}{E_{\mu}}\,\hat{\mathcal{P}}_{\mu,\mathrm{sf}}\right)\psi_{\mu}\ .$$

Omitting the second term on the right hand side of Eq.(13c) and introducing $\kappa = \frac{{}^{\mathcal{M}}\Lambda_{\mu}}{E_{\mu,0}}$ one arrives at

$$\left({}^{\mathcal{N}}\hat{H}_{\mu} \;+\; f\;{}^{\mathcal{M}}\hat{H}_{\mu}\,\hat{\mathcal{P}}_{\mu,\mathrm{sf}}\right)\psi_{\mu} = E_{\mu}\left(1 \;+\; \kappa\, f\,\frac{\mathcal{M}}{\mathcal{M}_{\mu}}\,\hat{\mathcal{P}}_{\mu,\mathrm{sf}}\right)\psi_{\mu}\ , \tag{36}$$

suggesting a geminal Hamiltonian expression

$$\hat{H}^{\mathrm{e}}_{\mu} = \left\{\left(1 + \kappa f\,\frac{\mathcal{M}}{\mathcal{M}_{\mu}}\hat{\mathcal{P}}_{\mu,\mathrm{sf}}\right)^{-1}\left({}^{\mathcal{N}}\hat{H}_{\mu} + f\,\left({}^{\mathcal{M}}\hat{H}_{\mu}\,\hat{\mathcal{P}}_{\mu,\mathrm{sf}}\right)^{s}\right)\right\}^{s} \tag{37}$$

with superscript s referring to symmetrization as before. A notable characteristic of $\hat{H}^{\mathrm{e}}_{\mu}$, as compared to $\hat{H}^{\mathrm{c}}_{\mu}$ and $\hat{H}^{\mathrm{d}}_{\mu}$ is that it involves $\hat{\mathcal{P}}_{\mu,\mathrm{sf}}$, yet its spin-pure limit in space R_{μ} is correct, though finding the limit is occasionally hampered by $\left(1 + \kappa f\,\frac{\mathcal{M}}{\mathcal{M}_{\mu}}\hat{\mathcal{P}}_{\mu,\mathrm{sf}}\right)$ being non invertible. See Appendix A in this respect.

Functions belonging to space Q_{μ} and to $\mu = V$ are orthogonal to those figuring in Eq.(11). Based on this, complete omission of the second and third terms on the right hand side of Eq.(12) is also warranted, resulting in the SLG counterpart of Eq.(12), ${}^{\mathcal{N}}\hat{H}_{\mu}$. This is applied in all PT variants reported in Section 4 for $\mu = V$. We mention that switching the operator of Eq.(35) to ${}^{\mathcal{N}}\hat{H}_{\mu}$ (or vica versa) in either space Q_{μ} or for $\mu = V$ has only a slight effect on energetic data.

Partitionings $1 - 3$ tested in this work, formulated with the effective Hamiltonians de-

scribed above, are summarized in Table 1.

Table 1: Partitioning variants tested in Sec. 4. Geminal subspaces involved in the reference correspond to $\mu \leq N/2$, the virtual subspace is indicated by $\mu = V = N/2 + 1$. Operators $\hat{H}^{\mathrm{b}}_{\mu}, \ldots, \hat{H}^{\mathrm{e}}_{\mu}$ are given in Eqs.(34), (32), (35) and (37).

	$1 \leq \mu \leq N/2$		$\mu = V$
partitioning	$\hat{H}^{R}_{\mu}$	$\hat{H}^{Q}_{\mu}$	$\hat{H}_{V}$
1	$\hat{H}^{\mathrm{c}}_{\mu}$	$\hat{H}^{\mathrm{b}}_{\mu}$	${}^{\mathcal{N}}\hat{H}_{V}$
2	$\hat{H}^{\mathrm{e}}_{\mu}$	$\hat{H}^{\mathrm{e}}_{\mu}$	
3	$\hat{H}^{\mathrm{d}}_{\mu}$	$\hat{H}^{\mathrm{d}}_{\mu}$	

In spin-pure situations $\hat{H}^{\mathrm{d}}_{\mu}$ falls back to ${}^{\mathcal{N}}\hat{H}_{\mu}$ since $f\mathcal{M} = 1$ and consequently $f\ \mathcal{M}_{\mu}\ {}^{\mathcal{M}}\hat{H}_{\mu} = {}^{\mathcal{N}}\hat{H}_{\mu}$ in such cases. The statement also holds for operator $\hat{H}^{\mathrm{e}}_{\mu}$. Variants 2 and 3 therefore provide the desired limit in the spin-pure case. We stress at this point that exact degeneracy of geminal states that initiated the development delineated in this section is resolved by all partitionings listed in Table 1. While quasi-degeneracy remains a potential risk, the effect did not show up in any variants and systems investigated in this work.

2.3.2 First order interacting space

The sum of geminal Hamiltonians form of Eq.(14) induces a product over fragments form of functions $\Psi^{(0)}_{K}$ used for expanding the first order correction, with fragments constructed with orbitals belonging to specific geminal subspaces. This allows for a categorization of functions $\Psi^{(0)}_{K}$, based on the number of geminals affected by excitation, the resulting number of electrons as well as the M_S value of affected subspaces. Functions $\Psi^{(0)}_{K}$ spanning the first order interacting space, i.e., having nonzero interaction with the reference are affected in at least two and in at most four geminals. The functions themselves can be depicted as given in Figs. 1. and 2. of Ref.,[74] when restricting geminal subspace dimensions to two. Unaltered part of the excited functions is derived from the geminal product $|\mathrm{SLG}\rangle$. The structure of the first order interacting space of the present PT scheme is exactly the same, as a result of the analogous definition of $\hat{H}^{(0)}$. Evaluation of the numerator of Eq.(24) necessitates two

extra terms for each $\Psi_K^{(0)}$ as compared to the formulation of Ref.[74] These are $\widetilde{H}_{0K}$ and M_{0K}, the expression of which are given in Appendix C.

Evaluation of the second order correction with strong symmetry forcing is more demanding since $\boldsymbol{G}$ has to be constructed in a space containing higher excitations than those contributing to Eq.(24). This is due to the fact that the spin-flip counterpart of $\psi_{\mu,0}$ is not an eigenfunction of $\hat{H}_\mu$. Higher excitations arise by M_S and particle number conserving excitations in geminals considered unaffected in Figs. 1. and 2. of Ref.[74] Excited states contributing to Eq.(25), lying out of the first order interacting space described in the previous paragraph can be categorized according to the number of 'excess' excited geminals. As this number grows, the contribution is expected to become less significant. Our applications resort to the case of just one 'excess' excited geminal in excitation case 3V of Ref.[74] This represents exact evaluation of Eq.(25) for the four-electron system of Section 4.1, while it provides an approximate version of $\mathcal{E}_{\rm s}^{(2)}$ for the other examples of Section 4.

Excitation in one geminal At difference with the PT scheme of Ref.,[74] excited states affected in just one geminal of $|\mathrm{SLG}\rangle$ may have nonzero first order coefficient since the corresponding inhomogeneous term of Eq.(18), H_{L0} is nonzero. (Note, that the variational problem is formulated for the projected geminal product while $|\mathrm{SLG}\rangle$ contributes to H_{L0}.) These states however remain non-contributing to the second order energy correction due to the generalized Brillouin-condition[24]

$$\langle \delta\mathrm{HP\text{-}SLG}\,|\,\hat{H} - E_{\rm HP}\,|\,\mathrm{HP\text{-}SLG}\rangle = 0\ . \tag{38}$$

To see this, write the numerator of Eq.(22) for term L picked from Eq.(16), resulting

$$\langle \mathrm{SLG}|(\hat{H} - E_{\rm HP})\hat{P}|\Psi_L^{(0)}\rangle\, c_L^{(1)} = \langle \mathrm{HP\text{-}SLG}|(\hat{H} - E_{\rm HP})|\Psi_L^{(0)}\rangle\, c_L^{(1)}\ . \tag{39}$$

Since $\Psi_L^{(0)}$ is a function covered by the first order variation denoted δHP-SLG in Eq.(38), the matrix element of Eq.(39) is zero. An analogous derivation reveals that such states do not contribute to the second order energy correction with strong symmetry forcing either.

2.3.3 Invariance to spin-flip in SLG

If a set of geminals ψ_μ is optimal by HP-SLG, then its spin-flipped counterpart is also optimal. Using the notation $\widetilde{\psi_\mu} := \hat{\mathcal{P}}_{\rm sf}\psi_\mu$, the product function

$$|\widetilde{\rm SLG}\rangle := \hat{\mathcal{P}}_{\rm sf}|{\rm SLG}\rangle = \prod_{\mu=1}^{N/2} \widetilde{\psi}_\mu^+|{\rm vac}\rangle \tag{40}$$

yields *the same* half-projected function (up to a sign) and the same point on the HP-SLG energy surface. It is desirable for a PT correction to be invariant to using either $|{\rm SLG}\rangle$ or $|\widetilde{\rm SLG}\rangle$ as reference. The PT schemes developed here possess this feature, as shown in Appendix B.

3 Computational details

In the applications of Section 4 the HP-SLG wavefunction is optimized with respect to geminal coefficients, but not with respect to orbitals. These are UNOs, more specifically, natural orbitals of the $M_S = 0$ UHF wavefunction, that underlie the calculations, similarly to Refs.[74,103] We use acronyms HP-USLG and USLG to refer to UNOs, that are in general not optimal orbitals of either HP-SLG or SLG. Geminal subspaces are determined by the pairing of UNOs according to their occupation number: if occupancy of an orbital is above a numerical threshold, it constitutes a one-dimensional geminal, while two-dimensional active geminals are constructed from UNO pairs with occupation numbers adding up to 2. In case of UNO occupation degeneracy we rely on Löwdin's pairing theorem[28,104] in assigning the proper alpha-beta pairs.

Both Ansätze are invariant under unitary transformation of doubly occupied orbitals, while the zero-order Hamiltonian does not exhibit this feature. To avoid any ambiguity, doubly occupied orbitals are pseudocanonicalized, meaning that they diagonalize the generalized Fockian

$$F_{ij} = 2h_{ij} + \sum_{kl} \gamma_{kl} \left[2[ik|jl] - [ik|lj]\right] \ , \tag{41}$$

where $\boldsymbol{\gamma}$ is the normalized one-particle reduced density matrix (1-RDM) of the respective wavefunction.

Computational cost of the approach deserves some remark. The time-determining step is the solution of the system of linear equations in Eq.(18), step count being determined by two factors: the number of blocks of coefficient matrix $\boldsymbol{G}$ and the size of individual blocks. The former depends on the number of fragments, while the latter is determined by dimension of geminal subspaces. For excited N-electron functions not involving the virtual subspace, dimension of a block is bounded by 16 from above, supposing at most two-dimensional non-virtual geminal subspaces. In these cases the number of blocks is the decisive factor, scaling as N_{gem}^4, with N_{gem} standing for the number of geminals. Regarding excited states with nonzero virtual geminal occupation, functions accommodating two electrons in the virtual space generate the most computational demand. Solving for the largest block of Eq.(18), having dimension $\sim N_{\text{virt}}^2$ scales as $N_{\text{virt}}^2 \times N_{\text{virt}}^2$, when performed efficiently. Since $N_{\text{gem}} << N_{\text{virt}}$ holds typically, the computational cost is $\mathcal{O}(N_{\text{gem}}^2 N_{\text{virt}}^4)$. Finally, the cost of additional spin projection needs to be mentioned. If weak symmetry forcing is applied, evaluation of Eq.(24) is of essentially the same cost as obtaining a second-order correction without spin projection, as construction of $\boldsymbol{G}$ and solution of Eq.(18) requires the same process as for USLGPT. There is one additional term arising in Eq.(24) arising from spin adaptation, that is $\widetilde{H}_{0K}$. Weak symmetry forcing therefore contributes a factor of two when computing the coupling matrix elements between excited states and the ground state. Since this is not the time-determining step of the computation, HP-USLGPT with the weak SAPT formalism is essentially of the same cost as USLGPT.

Excited states in general can not be expected to be represented well by geminal-based methods. The states contributing to the spin contaminated SLG and/or HP-SLG reference can however be assumed to be reliable. Lowest lying singlet and triplet states of radicaloids constitute a typical example, providing the test cases of Section 4. Control on the target state is achieved by choosing the appropriate geminal root in course of the variational optimization and by setting the value of parameter f accordingly. Geminal CI parameters characterizing the lowest singlet and triplet states at the level of the reference are collected in the Supplementary Material, together with the weights of separate spin components of the wavefunction.

Working PT formulae of the report are Eq.(24) and Eq.(25), labeled as 'w' and 's' for weak and strong respectively. The latter is evaluated approximately except for the case of Section 4.1. The zero order Hamiltonian entering the above expressions is one of the variants $1-3$ presented in a concise manner in Appendix A. Thus 'HP-USLG-PT2 3w' refers to Eq.(24) with $\hat{H}^{(0)}$ according to line three of Table 1.

Benchmarks are either provided by full CI (FCI) or by high accuracy theoretical data reported in the literature. Results by HP-USLG-PT are presented and discussed vis-à-vis USLG-PT, the main motive of the work being the amendment of the latter in case of severe spin contamination.

4 Results

4.1 H_4

Rectangle to square distortion of the H_4 system is investigated in the vicinity of the square geometry in 6-311G** basis. Note, that due to the unrestricted nature of the geminal reference, the cusp characteristic of singlet coupling at the square arrangement[105] is missing here. Ground state of the system by FCI is triplet in the geometry range investigated, with vertical excitation energy of the lowest lying singlet state falling between 7 mE_h and 31 mE_h.

When computed by USLG, the ground state is spin contaminated with total spin ranging from 1.43 to 1.80 when moving from rectangle to square geometry, while the singlet is spin-pure with correct spatial symmetry (A_g for rectangle and B_{2g} for square). Spin symmetry violation of the triplet USLG state is accompanied by spatial symmetry breaking. The picture is reversed in some sense for HP-USLG that results a triplet state both spin-pure and of correct spatial symmetry (B_{1g} for rectangle and A_{2g} for square). Aiming for the singlet, HP-USLG provides a solution of correct spatial symmetry and slightly spin contaminated (with $\langle \hat{S}^2 \rangle_{\text{HP-USLG}}$ falling between 0.03 and 0.04). Note, however, that spin contamination is marginal only after projection. The underlying geminal product function has more of a mixed character, as is apparent from Table 2, which contains spin component analysis of the geminal-based wavefunctions at two different geometries.

Table 2: Weight (in total coefficient squared sense) of $\hat{S}^2$-eigenfunctions corresponding to eigenvalue S in geminal-based wavefunctions, obtained for the singlet and triplet states of H_4 in 6-311G** basis, for selected geometries. For details see legend of Fig. 1.

		singlet state			triplet state		
		USLG	HP-USLG, before proj.	HP-USLG, after proj.	USLG	HP-USLG, before proj.	HP-USLG, after proj.
$\alpha = 85°$	$S = 0$	1	0.8477	0.9949	0.2906	0.1038	0
	$S = 1$	0	0.1480	0	0.7063	0.8443	1
	$S = 2$	0	0.0043	0.0051	0.0031	0.0519	0
	$\langle \hat{S}^2 \rangle$	0	0.3219	0.0304	1.4313	2.0000	2.0000
$\alpha = 90°$	$S = 0$	1	0.8314	0.9936	0.1031	0.1037	0
	$S = 1$	0	0.1632	0	0.8949	0.8444	1
	$S = 2$	0	0.0054	0.0064	0.0020	0.0519	0
	$\langle \hat{S}^2 \rangle$	0	0.3586	0.0384	1.8020	2.0000	2.0000

For a system built of two geminals, optimal CI coefficients of fragments are not unique[24] by HP-USLG. While this has no effect on the HP-USLG energy, PT corrections by Eq.(24) and Eq.(25) are affected since they are based on the unprojected function. Adopting the notation of Eq.(4), angles η_1 and η_2 are uniquely determined, while choice for δ_1 and δ_2 has one degree of freedom: for $f = 1$, $\tan(\delta_1) \cdot \tan(\delta_2) = K_1$ while for $f = -1$, $\tan(\delta_1)/\tan(\delta_2)$ has to be set to equal K_2 (constants K_1 and K_2 can be deduced from the CI expansion of the optimal HP-USLG wavefunction). To avoid any ambiguity, δ_1 and δ_2 are chosen to

fulfill the constraint above, and at the same time maximize the squared norm of the projected function. It can be shown that this choice results in $\delta_2 = \pm\delta_1$ for the singlet and $\delta_2 = \pm(\pi/2 - \delta_1)$ for the triplet (sign of δ_1 and δ_2 depending on the sign of K_1 and K_2, respectively). This choice is reasonable since unwanted components of the unprojected function are of the smallest possible norm, a situation preferable for HP-SLG-PT as underlined by the results in Sec. 4.2.1. Spin component data of the HP functions in Table 2 correspond to the wavefunctions parametrized accordingly.

Energies and singlet-triplet splittings for a few selected geometries obtained by HP-USLG-PT2 are collected in Table 3, complemented by unperturbed data and USLG-PT2. Energy gaps of the references providing zero-order approximation to the wavefunction, USLG and HP-USLG are both found to give overestimates as compared with the FCI data in Table 3. Results by HP-USLG are only slightly better than those by USLG.

Second order geminal PT based on USLG yields poor results, even reversing the order of singlet and triplet for $\alpha = 85°$. Examining the error of individual states shown in Figs. 1 and 2, the error of USLG-PT2 is found to be between 5 mE_h and 10 mE_h for the singlet and around 20 mE_h for the triplet. The source of poor performance of geminal PT based on USLG is accordingly an imbalanced treatment of singlet and triplet-like reference states, as has been observed in connection with UMP[17] when the system has a triplet ground state.

In comparison, projected PT applied to HP-USLG brings a substantial improvement to energy differences, if the partitioning is chosen appropriately. As seen in Table 3, HP-USLG-PT2 variants 1 and 2 perform better than USLG-PT2, but they still underestimate the singlet-triplet gap. A look at individual energies in Figs. 1 and 2 reveals that both states are characterized by a larger error than USLG-PT2 and an imbalance remains in that the triplet exhibits larger error by HP-USLG-PT2 1, than the singlet. It may appear disturbing, that singlet energies by USLG-PT2 and HP-USLG-PT2 are markedly different even though both states are essentially spin-pure. This can be argued with the nonnegligible spin contamination of the zero-order of the HP-USLG-PT2 scheme, i.e. the geminal product underlying

HP-USLG, cf. Table 2. Variant 3 of HP-USLG-PT2 is more successful in predicting the gap, notably because it does not increase the error of USLG-PT2 for the triplet, cf. Fig. 1, it merely flattens the error curve. Based on Table 3, HP-USLG-PT2 variant 3 can estimate the singlet-triplet gap with an error of 5-15 % even though energetic description of the individual states is not highly accurate. In our experience, HP-USLG-PT2 energy contributions are in general suppressed compared to USLG-PT2. In the present example a smaller PT2 energy contribution to the singlet HP-USLG solution brings forth a more balanced description of states. The geminal product states underlying the HP-USLG wavefunction have a similar amount of spin contamination for the singlet and triplet roots in the sense that weight of the target component is around 0.85 for both states. The case of USLG is less balanced, this weight being 1.0 for the singlet, and only 0.71 for the triplet. Energy gaps shown in Fig. 3 complement the picture: the farther the geometry gets from square the closer HP-USLG-PT2 gets to FCI.

A few words are now due on the performance of different partitionings in Table 3. Variant 2 is seen to be more accurate than variant 1, achieving a shift of total energies in the correct direction, and improving gaps too. The numerical difference can be mainly attributed to $\hat{H}^{\mathrm{b}}_{\mu}$ in space Q_{μ} being replaced by $\hat{H}^{\mathrm{e}}_{\mu}$ in variant 2 and implies that the latter is more successful. Results by 2 fall between 1 and 3. Difference between variants 2 and 3 signifies that $\hat{H}^{\mathrm{d}}_{\mu}$ is even more fortunate in space Q_{μ} than $\hat{H}^{\mathrm{e}}_{\mu}$.

Data in Table 3 also serves for comparison of weak and strong symmetry forcing, cf. Eqs.(24) and (25), revealing that altering the partitioning may have larger effect than changing the symmetry forcing strategy. Gaps are only slightly changed when comparing weak and strong versions of the same HP-USLG-PT2 variant. According to expectations, difference between weak and strong symmetry forcing is found to be more pronounced in numerical terms for larger systems, vide infra.

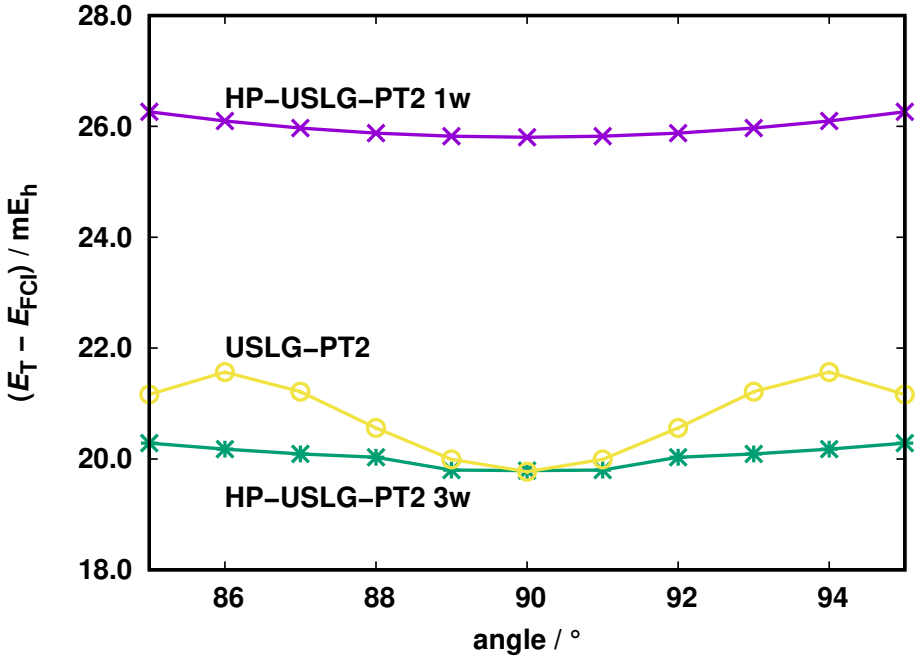

Figure 1: Energy error (relative to FCI, given in mE_h) for the triplet state of the H_4 molecule in 6-311G** basis, obtained by geminal-based models. The H atoms form the vertices of a rectangle, moving on a circle of 1.0 bohr radius. With X denoting the centre of mass, the angle $\alpha = \angle(\mathrm{HXH})$ is varied.

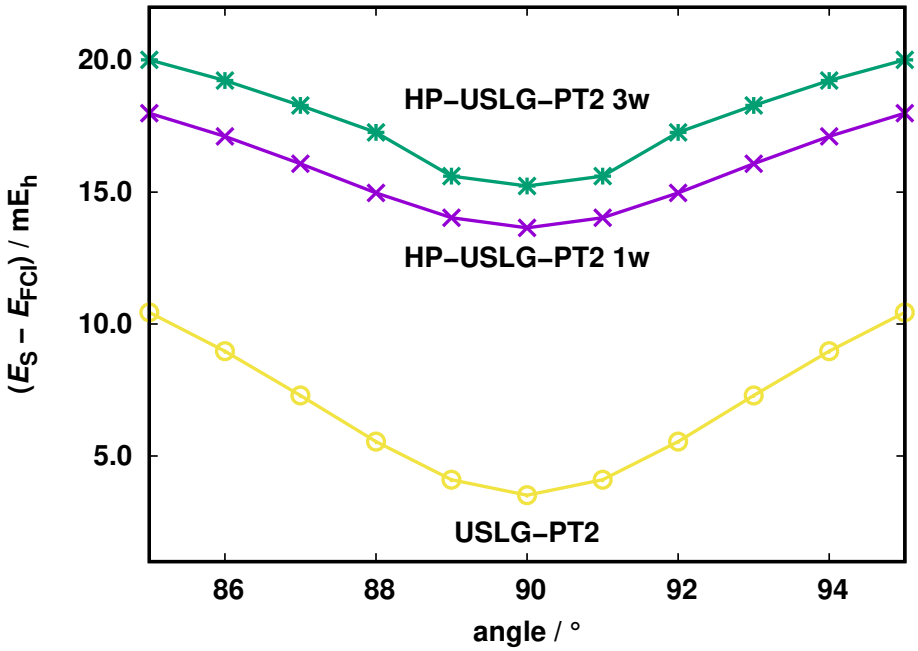

Figure 2: Energy error (relative to FCI, given in mE_h) for the singlet state of the H_4 molecule in 6-311G** basis, obtained by geminal-based models. For further details see the legend of Fig. 1.

Table 3: Total energy of the triplet state (given in E_h) and singlet-triplet gap ($\Delta E = E_S - E_T$, in mE_h) of the H_4 molecule in 6-311G** basis, obtained by geminal-based models. See the legend of Fig. 1 for geometry. Benchmark is provided by FCI.

	α / °					
	85		87		90	
method	E_T	ΔE	E_T	ΔE	E_T	ΔE
USLG	−1.863433	20.41	−1.863819	31.08	−1.864476	39.53
USLG-PT2	−1.907742	−3.59	−1.909983	6.52	−1.912708	14.58
HP-USLG	−1.871671	18.72	−1.874354	30.36	−1.875856	38.30
HP-USLG-PT2 1w	−1.902642	−1.15	−1.905227	10.54	−1.906674	18.68
HP-USLG-PT2 1s	−1.901692	−1.01	−1.904286	10.56	−1.905741	18.50
HP-USLG-PT2 2w	−1.906081	2.669	−1.908614	14.25	−1.910031	22.29
HP-USLG-PT2 2s	−1.905021	2.709	−1.907566	14.18	−1.908993	22.03
HP-USLG-PT2 3w	−1.908620	6.854	−1.911105	18.63	−1.912689	26.28
HP-USLG-PT2 3s	−1.907585	6.869	−1.910085	18.53	−1.911389	25.99
FCI	−1.928906	7.13	−1.931197	20.44	−1.932478	30.84

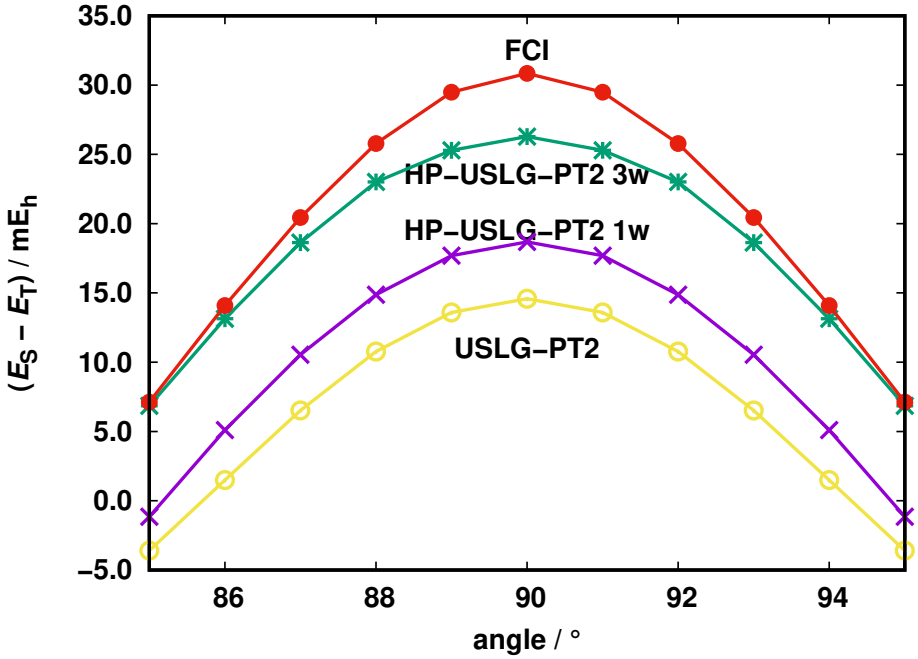

Figure 3: Vertical excitation energies ($E_{\mathrm{S}} - E_{\mathrm{T}}$, in $\mathrm{mE_h}$) of the H_4 molecule in 6-311G** basis, obtained by geminal-based models. Benchmark is provided by FCI. For details on geometry see Fig. 1.

4.2 Diatomic molecules

4.2.1 O_2

Singlet-triplet splitting is computed for the oxygen molecule in 6-31G basis. At the geometries taken from experiment UHF is spin contaminated, with two occupation numbers being 1.00 for the π-type bonding UNOs. In addition to this, two more geminals are correlated, corresponding to the π-type lone pairs of the oxygens. Apart from the orbitals assigned to these three geminals, all other UNOs (occupation number greater than 1.998) are considered doubly occupied and are pseudocanonicalized.

Starting with USLG, both states are found spin-pure,[74] energy gaps by USLG-PT2 are accordingly expected to be adequate. The energy error of the USLG-PT2 gap is in fact 4% as compared with FCI, as shown in Table 5. Since no spin contamination appears at the level of USLG, it can not be claimed as a drive for computing HP-USLG, which is examined in this situation in order to gain experience.

Distinct solutions are found for HP-USLG for both states, slightly spin contaminated and slightly below USLG in energy, by cca. 5.5 $\mathrm{mE_h}$, cf. Table 5. The triplet HP-USLG solution is characterized by $\langle \hat{S}^2 \rangle_{\text{HP-USLG}} = 2.000$, and $\langle \hat{S}^2 \rangle_{\text{HP-USLG}} = 0.017$ stands for the singlet. Optimal geminal parameters collected in Table 4 reveal the difference in the HP-USLG solutions compared to USLG, that is rather imperceptible when looking at total spin. Examining the parameters in Table 4, the two lone pair geminals are essentially found singlet for all methods and states (δ_1 and δ_2 being close to zero). Total spin of the product is therefore determined essentially by the bonding geminal.

For HP-USLG, a peculiar phenomenon can be observed: the geminal product function of the singlet state has more of a triplet character, since δ_3 in Table 4 is closer to 90° than to zero. Weight of the components (in coefficient squared sense) with even S is consequently less than that of the unwanted, odd S components. This results in a negative value for $\mathcal{M}$ (cca. -0.79). Multiplied by $f = 1$ corresponding to projection to singlet and plugged in

Eq.(8), a rather small value is obtained which in turn contributes the denominator to Eq.(24). The case of the triplet state is completely analogous: the bonding geminal is mainly singlet in HP-USLG (δ_3 in Table 4 is small), resulting in $\mathcal{M} \approx 0.79$, which, combined with $f = -1$ once again yields a small denominator in Eq.(24). Though the wavefunction is normalized after projection, such zero-order states can undermine the performance of SAPT since it relies on the unprojected reference.

Table 4: Optimal geminal parameters (δ, η in degrees) and corresponding quantities for the O_2 molecule in 6-31G basis.

triplet			
μ	1	2	3
δ_μ, USLG	0.00	0.00	90.00
η_μ, USLG	1.39	1.39	n.a.
δ_μ, HP-USLG	0.88	0.88	18.86
η_μ, HP-USLG	1.44	1.44	45.00
$\mathcal{M}_\mu$, HP-USLG	0.9995	0.9995	0.7910
singlet			
μ	1	2	3
δ_μ, USLG	0.00	0.00	0.00
η_μ, USLG	1.35	1.35	45.00
δ_μ, HP-USLG	0.90	0.90	71.20
η_μ, HP-USLG	1.40	1.40	45.00
$\mathcal{M}_\mu$, HP-USLG	0.9995	0.9995	−0.7922

The effect of projecting in the "wrong direction" manifests both in total energies and gaps by HP-USLG-PT2 in Table 5. A small denominator in Eq.(24), if not counteracted by a similarly small numerator, results in a large second order correction in absolute value. This is the reason for HP-USLG-PT2 energies getting way below FCI (variants 1 and 2). Even though variant 2 shifts energies closer to FCI for both states, the adiabatic gap is improved only slightly compared to 1. Variant 3 performs better in this regard, however, the adiabatic excitation energy by HP-USLG-PT2 remains essentially of the same quality as HP-USLG.

Concluding this example, a couple of milihartrees energy lowering at the level of HP-USLG induces a significant change in the geminal product wavefunction, raising the weight of the unwanted spin component above that of the target component. Projected PT schemes

Table 5: Energy of the triplet ground state and first excited singlet state of the oxygen molecule (in E_h) in 6-31G basis. Energy difference $\Delta E = E_S - E_T$ is given in mE_h. Geometries are taken from Ref.[106] as $R_S = 1.21563$ Å and $R_T = 1.20752$ Å. The 1s core orbitals of the oxygen atoms are frozen in FCI calculations.

method	E_T	E_S	ΔE
USLG	−149.531307	−149.497527	33.78
USLG-PT2	−149.739058	−149.699740	39.32
HP-USLG	−149.536840	−149.503014	33.84
HP-USLG-PT2 1w	−149.863768	−149.724597	139.2
HP-USLG-PT2 2w	−149.820329	−149.725780	94.55
HP-USLG-PT2 3w	−149.760113	−149.729031	31.08
FCI	−149.784823	−149.744266	40.56

that apply symmetry projection along with composing the correction become unreliable in such a situation.

4.2.2 NH

Similarly to the oxygen molecule, the ground state of the NH molecule is triplet ($^3\Sigma$), and the lowest lying singlet state ($^1\Delta$) is multiconfigurational. Single-reference methods consequently miss a significant amount of correlation for the singlet state, and therefore overestimate the singlet-triplet gap.[98]

Calculations are carried out in cc-pVTZ basis[107] to allow comparison to data of Ref.[108] Geometries of the two states are based on experiment. For both interatomic distances, the $M_S = 0$ UHF solution is strongly spin contaminated with $\langle \hat{S}^2 \rangle_{\text{UHF}} \approx 1.01$. All valence electrons (altogether 6 electrons in 3 geminals) are correlated in geminal computations. Occupation number threshold separating the doubly occupied orbitals from active UNOs is 1.9999 in this case. Both the ground state and the singlet excited state can be described by USLG in a spin-pure manner. Similarly to the case of O_2, stepping to HP-USLG does not appear an absolute must. Investigating half-projection nonetheless, distinct HP-USLG solutions of cca. 10 mE_h below USLG are found, characterized by a total spin value 2.00 for the triplet and $\langle \hat{S}^2 \rangle_{\text{HP-USLG}} = 0.02$ for the singlet. In contrast with O_2, the geminal product underlying HP-USLG exhibit proper spin character for both states, meaning that

the singlet weight is most pronounced for even S, and the product is dominantly triplet for odd S. Individual spin components listed in the Supplementary Material reveal that while the triplet HP-USLG wavefunction is essentially spin-pure, the geminal product underlying HP-USLG is spin contaminated, though dominantly triplet. Based on this, a breakdown of HP-USLG-PT, similar to that seen in Section 4.2.1 is not anticipated on this example.

Table 6: Total energy of the triplet state of the NH molecule in cc-pVTZ basis (E_{T}, in $\mathrm{E_h}$). Adiabatic singlet-triplet gaps ($E_{\mathrm{ST}} = E_{\mathrm{S}} - E_{\mathrm{T}}$) are given in kcal/mol. Bond lengths are $R_{\mathrm{S}} = 1.034$ Å and $R_{\mathrm{T}} = 1.036$ Å, based on Ref.[106]

method	E_{T}	ΔE_{ST}
USLG	−54.973483	40.8
USLG-PT2	−55.092502	34.3
HP-USLG	−54.983334	40.4
HP-USLG-PT2 1w	−55.071873	26.0
HP-USLG-PT2 2w	−55.079467	30.8
HP-USLG-PT2 3w	−55.087020	36.2
CASPT2(2,2)[2]		36.5
CASPT2(FV)[2]		37.0
EMP2(0)[2]		35.8
EMP2[2]		35.7
SUPT2[2]		36.7
SF-OD[1]		38.2
expt.[3]		35.93

[1] Ref.[108]
[2] Ref.[97]
[3] Ref.[106]

Adiabatic gaps by HP-USLG-PT2 as well as other perturbative methods are collected in Table 6. Energetic values by spin-flip EOM-CCD with optimized orbitals, obtained with the same basis and geometry, labeled SF-OD can be regarded as benchmark in Table 6, experimental gap is shown for reference. Gaps by geminal models USLG and HP-USLG largely agree in providing an overestimation, HP-USLG being only slightly better than USLG. Correction by second order PT invariably reduces the gap. An excessive effect can be observed with variants 1, 2 that were found relatively poorly performing in Section 4.1 too. The gap by USLG-PT2 is also worse than the reference USLG, when compared to SF-OD. Partitioning 3 improves upon USLG-PT2 in a way similar to that seen in Section 4.1: PT correction

of the triplet is slightly, that of the singlet is more considerably shrunk, compared to USLG-PT. This results in the cca. 10% error of the USLG-PT2 gap diminished to around 5% by HP-USLG-PT2 in partitioning 3. The observation of Section 4.1 applies here too in that HP-USLG-PT2 individual energies are worse than USLG-PT2 estimates, while gaps are more reliable by HP-USLG-PT2 with a well chosen partitioning.

Gaps by HP-USLG-PT2 also compare more favourably with experiment, though this observation may be biased by definition issues of the energy of transition by experiment. Gaps by HP-USLG-PT2 in partitioning 3 are similar to PT corrected values of fully projected single determinant schemes, EMP2 and SUPT2. These latter as well as CASPT2 correspond to a significantly larger basis (aug-cc-pVQZ),[97] comparison is hence not completely appropriate.

4.3 O_3

Ozone is a popular test system of multireference approaches both in its ground and excited states.[109–112] While a large amount of experimental data is available, reproducing these by theoretical methods remains a challenging task, necessitating a careful, balanced treatment of static and dynamic correlation, as pointed out by Gauss and coworkers.[113]

We investigate the singlet ground state and the lowest lying triplet state in cc-pCVDZ basis.[114] The C_{2v} equilibrium geometry of the ground state is employed with parameters borrowed from Ref.[113] Vertical excitation energies obtained by geminal-based methods are benchmarked against high accuracy linear response based on singles, doubles and full triples involving CC (CCSDT-LR), cited from Ref.[113] Results of CCSD based LR are also shown for reference in Table 7.

The $M_S = 0$ UHF solution is highly spin contaminated with $\langle \hat{S}^2 \rangle_{\mathrm{UHF}} = 0.95$. Total spin is considerably improved at the USLG level, yielding $\langle \hat{S}^2 \rangle_{\mathrm{USLG}} = 0.014$ for the singlet type root, when correlating six geminals. Two of the correlated geminals are of π character, and the other four are built with orbitals of σ symmetry. Occupation number threshold

for doubly occupied orbitals is 1.9996. Singlet part of the most correlated geminal is of $^1A_1$ symmetry, while its triplet component can be described as $^3B_2$. Spin contamination is therefore necessarily accompanied by spatial symmetry violation. The triplet state is both spin-pure and of correct spatial symmetry by USLG. In comparison, HP-USLG is slightly contaminated for both states, resulting $\langle \hat{S}^2 \rangle_{\text{HP-USLG}} = 0.023$ for the singlet, and 2.001 for the triplet solution. While the slight spin violation persists, spatial symmetry of the singlet root is fully restored by HP, and is not spoiled for the triplet root either.

Perturbative corrections based on geminal reference functions are displayed in Table 7. Total spin being satisfactory by USLG, PT formulation of Ref.[74] is fairly adequate and serves as a good basis of comparison for HP-USLG-PT variants.

Table 7: Ground state energy (in E_h) and vertical excitation energy (in eV) of the lowest triplet state of the ozone molecule in cc-pCVDZ basis, obtained by different geminal based models. Single-reference CC based linear response calculations are cited as benchmark. Symmetry of the molecule is C_{2v} with parameters taken from Ref.[113] as $R_{\text{O–O}} = 1.2569$ Å and $\angle(\text{OOO}) = 116.54°$.

	$^1A_1$	$^3B_2$
USLG	−224.3653	0.977
USLG-PT2	−224.8791	1.503
HP-USLG	−224.3746	0.937
HP-USLG-PT2 1w	−224.8714	2.426
HP-USLG-PT2 2w	−224.8659	1.956
HP-USLG-PT2 3w	−224.8651	1.464
HP-USLG-PT2 3s	−224.8081	1.720
CCSD-LR[1]	−224.9981	1.421
CCSDT-LR[1]	−225.0311	1.716
expt.[2]		1.29

[1] Ref.[113]
[2] Ref.[115]

A considerable underestimation of the gap can be observed in Table 7, at the level of reference. Accepting CCSDT-LR as the best theoretical estimate in Table 7, USLG based PT schemes bring significant improvement.

In accord with all other cases investigated, suppressed energy corrections by HP-USLG-PT are apparent in Table 7 when comparing total energies with that of USLG-PT. The effect

varies both with partitioning scheme and the state in question, resulting diverse values for the gap. Schemes denoted 1w and 2w are seen to give an overcorrection when compared with the gap of CCSDT-LR. The success of HP-USLG-PT partitioning 3 is comparable to USLG-PT in predicting the gap when applying weak symmetry forcing. As anticipated, difference between weak and strong symmetry adaptation is more pronounced on this example, than for the H_4 system, albeit strong symmetry forcing is evaluated with approximations, cf. Sec. 2.3.2. Results by 3s represent the most reduced PT correction regarding individual state energies while the gap is more in line with CCSDT-LR when compared with its weak counterpart. Similarly to the case of the NH molecule, partitioning 1 results an overcorrection of the gap, while partitioning 2 falls in between 1 and 3.

Investigations with 4 correlated geminals, reported in the Supplementary Material, reflect similar tendencies.

4.4 *Para*-benzyne

Diradical character of benzyne isomers increases in the order of *ortho*, *meta*, *para*, which is accompanied by decreasing singlet-triplet gaps in the same order. Though UHF is heavily spin contaminated for all isomers, geminal coefficient optimization yields spin-pure USLG solutions with the exception of the singlet state of *para*-benzyne, for which $\langle \hat{S}^2 \rangle_{\mathrm{USLG}} = 1.05$. For this solution, spin contamination is accompanied by breaking of spatial symmetry at the level of the many-electron state.

Adiabatic excitation energies by USLG are of correct sign and order of magnitude. Incorporating dynamic correlation by means of PT further improves gaps.[74] The only exception is the *para* isomer, for which USLG-PT2 provides incorrect energetic estimates, reversing the order of the singlet and triplet states. Poor performance of USLG based PT for *para*-benzyne has been linked to the spin contamination of the reference, providing the chief motive in developing HP-USLG based PT.

Computational details and geometry are the same as in Ref.,[24] 6-31G* basis set is em-

ployed. Four geminals are correlated both at the USLG and at the HP-USLG level: three of them are built with π orbitals of the carbon atoms, while the fourth consists of σ orbitals responsible for the diradical character.

Previous results[24] at the level of HP-USLG were encouraging yet unsatisfactory since HP was successful at removing most of the spin contamination, adiabatic gap for *para*-benzyne however deteriorated as compared to USLG. By restoring spin symmetry of the geminal reference partially, spatial symmetry is fully recovered for both states. The reason behind is that singlet component of the correlated geminals corresponds to ^1A_g while triplet components are described as $^3B_{1u}$ in the D_{2h} point group. Consequently, product of an even number of triplets is of ^1A_g symmetry, while an odd number of triplets results in $^3B_{1u}$. Half-projection removes completely the $^3B_{1u}$ component of the product for $f = 1$ and the ^1A_g component is eradicated for $f = -1$.

Total energies, adiabatic gaps as well as spin expectation values are collected in Table 8 for the *para* isomer. Results by spin-flip EOM-CCD with optimized orbitals,[108] denoted SF-OD in Table 8 serve as benchmark. Experimental gap is indicated for reference.

As Table 8 reflects, PT based on the partially spin-purified geminal reference successfully amends the qualitative failure of USLG-PT. Ordering of the states and magnitude of the gap is correct by HP-USLG-PT2 in any of the partitionings. Comparing the performance of different HP-USLG-PT2 variants, trends are similar to those observed in previous test cases. Second order energy is suppressed by HP-USLG-PT2 when compared with USLG-PT and the effect is more sizeable for strong symmetry forcing. Regarding the gaps, partitionings 1 and 2 are rather similar. Focusing on weak symmetry forcing, 1w and 2w overestimate the adiabatic gap, by cca. 40-50%, taking SF-OD as benchmark. Variant 3w provides an estimation from the other side, underestimating the gap by cca. 30%.

Strong symmetry forcing uniformly increases the gap, deteriorating the performance of variants 1 and 2. At the same time, gap by 3s is remarkably in line with SF-OD (being in cca. -4% error) and falls within the error margin of the experimental value.

Table 8: Total energy of the ground state (in E_h) and adiabatic gap (in eV) of *para*-benzyne in 6-31G* basis. Geometries and SF-OD values are taken from Ref.[108] Spin expectation value of geminal based references is also tabulated. (Carbon-carbon distance of 1.4186 Å for the triplet state of *para*-benzyne is clearly in error in Ref.[108] Based on the nuclear repulsion data, this parameter is corrected for 1.367 Å.)

method	^1A_g	$^3B_{1u}$
USLG	−229.422647	0.139
USLG-PT2	−229.972968	−0.290
HP-USLG	−229.438909	−0.004
HP-USLG-PT2 1w	−229.962303	0.264
HP-USLG-PT2 1s	−229.833469	0.281
HP-USLG-PT2 2w	−229.958385	0.240
HP-USLG-PT2 2s	−229.830363	0.261
HP-USLG-PT2 3w	−229.948724	0.121
HP-USLG-PT2 3s	−229.822766	0.167
SF-OD[a]	−230.15415	0.174
expt.[b]		0.165 ± 0.016
$\langle \hat{S}^2 \rangle_{\text{USLG}}$	1.05	2.00
$\langle \hat{S}^2 \rangle_{\text{HP-USLG}}$	0.25	2.17

[a] Ref.[108]
[b] Ref.[116]

5 Conclusion

While shortcomings of the singlet coupled geminal product Ansatz can be rectified by allowing geminals to get spin-mixed, spin contamination of the resulting many-electron function may undermine dynamical correlation schemes built upon it. At the same time, geminal product structure of the reference is advantageous from the point of view of PT, allowing for a zero-order Hamiltonian composed as a sum of geminal Hamiltonians, incorporating intrageminal correlation. This PT technique can not be applied straightaway when spin contamination of the reference is cured by projection operators, since the resulting *sum* of geminal products is not an eigenfunction of a sum of geminal Hamiltonians construction. Performing spin-symmetry adaptation along with composing the correction terms by PT is a workaround developed and tested in this study.

Partial restoration of spin symmetry is performed at the level of reference, adopting a

variation after projection scheme regarding CI coefficients of the strongly orthogonal geminal Ansatz. In principle, orbitals can also be subjected to optimization, though for the time being they are conserved as natural orbitals of the UHF wavefunction. Orbital subspaces are here determined based on the pairing of UNOs, they are consequently at most two-dimensional.

Symmetry adapted PT is applied in two schemes, either with weak or with strong symmetry forcing. The zero-order reference is provided by the geminal product underlying the variationally optimized HP-USLG function. Half-projected energy corresponding to the variational solution is recovered at order one in energy. First order correction to the wavefunction utilizes the geminal eigenvalue equation arising from the energy optimum condition of HP-USLG. Several variants for the effective geminal operators contributing to the zero-order Hamiltonian are tested, differing in the effect on geminal states not contributing to the geminal product.

Numerical comparison of PT formulations reveals a general picture of suppressed second order energy correction by symmetry adapted PT juxtaposed USLG based PT, the latter lacking any treatment of spin symmetry. This applies to all partitioning variants (admittedly at a varied extent) and can be attributed to the SAPT formalism, i.e. to the second and third terms in the numerator of Eq.(24) when adopting weak symmetry forcing. First order coefficients $c_K^{(1)}$ are largely in line by symmetry adapted PT and USLG based PT. Strong symmetry forcing is evaluated in an exact manner for the H_4 system. For this system shrinking of the PT correction is more expressed by strong symmetry forcing than by the weak scheme. The statement also holds for the cases of Sec. 4 where strong symmetry forcing is evaluated in an approximate manner. Contributions neglected in Eq.(25) can be shown to be of negative sign, lifting the approximation is therefore expected to get total energies in strong symmetry forcing closer to those by the weak scheme.

Singlet-triplet gaps evaluated in the test cases are quite sensitive to the correction of the individual states. Gaps by HP-USLG-PT generally improve upon the value obtained at the level of HP-USLG. The results are qualitatively similar to USLG-PT2 when half-projection

has a marginal effect on the reference function (e.g. the case of NH and O_3). Gaps are considerably improved by HP-USLG-PT2 as compared with USLG-PT2 when significant spin contamination affects USLG (e.g. the case of H_4 and *para*-benzyne). We report failure of HP-USLG-PT2 as compared to USLG-PT2 when half-projection introduces a significant spin contamination at the level of the geminal product as compared to USLG (cf. the case of O_2). This situation is easily identified as it involves projection in the "wrong direction" in course of the PT procedure, accompanied by relatively small norm of the projected geminal product.

Of the partitionings tested in this work, variant 2 involves the least modification starting from the HP-USLG geminal eigenvalue equation, regarding excited subspaces R_μ and Q_μ. This variant is usually outperformed by 3. Main difference between variant 2 and 3 is the complete omission of the local spin-flip divided by $\mathcal{M}_\mu$. Results by HP-USLG-PT are most sensitive to the definition of the zero-order in excited space Q_μ and for the virtual orbital subspace $\mu = V$. Geminal Hamiltonian $\hat{H}^d_\mu$ performs rather similarly to the USLG limiting expression ${}^{\mathcal{N}}\hat{H}_\mu$ both in space Q_μ and for $\mu = V$. Applying the level-shifted Hamiltonian $\hat{H}^b_\mu$ instead of $\hat{H}^d_\mu$ in space Q_μ is usually accompanied by a deterioration of the gap values as reflected by the comparison of variants 1 and 3.

Of the partitionings tested in this work, variant 3 may be suggested as a well performing method, free from the occasionally ill-defined division or inversion, discussed in Appendix A.

Acknowledgement

Financial support in the framework of the ÚNKP-20-4 New National Excellence Program provided by the Hungarian Ministry for Innovation and Technology from the source of the National Research, Development and Innovation Fund is acknowledged by Zs.É.M. The work was completed in the ELTE Institutional Excellence Program (TKP20 20-IKA-05) financed by the Hungarian Ministry of Human Capacities.

The Supporting Material of this work includes geminal coefficient parameters as well as spin components of reference functions at various levels (USLG, HP-USLG and USLG underlying HP-USLG). This is available free of charge via the Internet at `http://pubs.acs.org`

A Partitionings used in the PT scheme

A.1 Local spin-flip

Derivation of Eq.(12) involves $M_S = 0$ geminal states with two electrons, whereas in the PT development $M_S \neq 0$ two-electron states also occur, moreover geminals occupied by zero, one, three and four electrons show up as well. This raises a question on the effect of $\hat{\mathcal{P}}_{\mu,\mathrm{sf}}$. Adopting the straightforward definition in Eq.(12) that $\hat{\mathcal{P}}_{\mu,\mathrm{sf}}$ flips all alpha spins to beta and vica versa in subspace μ (up to a sign), and substituting it in Eq.(14) leads to $[\hat{H}^{(0)}, \hat{S}_z] \neq 0$. When the first order correction, $|\Psi^{(1)}\rangle$ is obtained in this way, it violates $\hat{S}_z$. Since $|\mathrm{SLG}\rangle$ can be characterized by $M_S = 0$, the $M_S \neq 0$ components of an $\hat{S}_z$-violating $|\Psi^{(1)}\rangle$ are noninteracting through $\hat{H}$ and can not have a direct contribution to the second order energy. An indirect effect through values of $c_K^{(1)}$ is however possible. This is considered undesirable and a definition of $\hat{\mathcal{P}}_{\mu,\mathrm{sf}}$ according to Ruiz[102] is adopted in order to avoid this situation. In the spirit of Ref.[102] $\hat{\mathcal{P}}_{\mu,\mathrm{sf}}$ is defined as flipping the spin of $\min(k,l)$ electrons, in all possible ways in subspace μ. Here k is the number of electrons with alpha spin, l is the number of electrons with beta spin occupying orbitals in *subspace* μ. The effect of $\hat{\mathcal{P}}_{\mu,\mathrm{sf}}$ is similar to Eq.(6) in other respects. To be more specific, taking a determinant with k alpha and l beta electrons ($k \geq l$) in subspace μ, we have for $i_1, \ldots, i_l, j_1, \ldots, j_k \in \mu$

$$\hat{\mathcal{P}}_{\mu,\mathrm{sf}}\; i^+_{1\beta} \ldots i^+_{l\beta} j^+_{1\alpha} \ldots j^+_{k\alpha} |\phi\rangle = (-1)^l \sum_{1 \leq t_1 < \ldots < t_l \leq k} i^+_{1\alpha} \ldots i^+_{l\alpha} j^+_{1\alpha} \ldots j^+_{t_1\beta} \ldots j^+_{t_l\beta} \ldots j^+_{k\alpha} |\phi\rangle \;. \quad \text{(A.1)}$$

In the above, $|\phi\rangle$ is the part of the determinant not involving orbitals from subspace μ and left intact by $\hat{\mathcal{P}}_{\mu,\mathrm{sf}}$. The effect of $\hat{\mathcal{P}}_{\mu,\mathrm{sf}}$ is completely analogous to $\hat{\mathcal{P}}_{\mathrm{sf}}$ when $k = l$, in particular

$$\hat{\mathcal{P}}_{\mu,\mathrm{sf}}\,|^1\psi_\mu\rangle = \ |^1\psi_\mu\rangle \tag{A.2a}$$

$$\hat{\mathcal{P}}_{\mu,\mathrm{sf}}\,|^3_0\psi_\mu\rangle = \ -\,|^3_0\psi_\mu\rangle \tag{A.2b}$$

$$\hat{\mathcal{P}}_{\mu,\mathrm{sf}}\,|^3_{-1}\psi_\mu\rangle = \ |^3_{-1}\psi_\mu\rangle \tag{A.2c}$$

$$\hat{\mathcal{P}}_{\mu,\mathrm{sf}}\,|^3_1\psi_\mu\rangle = \ |^3_1\psi_\mu\rangle \tag{A.2d}$$

where ${}^1\psi_\mu$, ${}^3_0\psi_\mu$, ${}^3_{-1}\psi_\mu$ and ${}^3_1\psi_\mu$ are singlet, triplet $M_S = 0$, triplet $M_S = -1$ and triplet $M_S = 1$ two-electron functions, respectively. An $M_S = \pm 1/2$ one-electron state in subspace μ is also left intact by $\hat{\mathcal{P}}_{\mu,\mathrm{sf}}$, while it transforms a three-electron fragment as

$$\hat{\mathcal{P}}_{\mu,\mathrm{sf}}\; i^+_\beta j^+_\alpha m^+_\alpha|\phi\rangle = \ -\,i^+_\alpha j^+_\beta m^+_\alpha|\phi\rangle - i^+_\alpha j^+_\alpha m^+_\beta|\phi\rangle\ . \tag{A.3}$$

In the case of two-dimensional geminal subspaces, as occurs in this work for $\mu \neq V$, the effect of $\hat{\mathcal{P}}_{\mu,\mathrm{sf}}$ in Eq.(A.3) is found to be the unit operator, since either $i = j$ or $i = m$.

A.2 Geminal energies by Eq.(12) in the spin-pure limit

As discussed in Sec. 2.3.1, eigenstates of $\hat{H}^{\mathrm{eff}}_\mu$ of Eq.(27) match those of ${}^{\mathcal{N}}\hat{H}_\mu$ in the spin-pure limit, but energy differences are not the same. Appearance of spin-flip terms causes an artificial shift in geminal energies that is pinpointed below for functions of space R_μ.

In order to evaluate the effect of Eq.(27), the spin-pure limit of $\mathcal{M}_\mu = \cos(2\delta_\mu)$ and $\mathcal{M}$ of Eq.(9) is to be set. For the singlet, $\delta_\mu = 0$ in Eq.(4), therefore $\mathcal{M}_\mu = 1$, while $\mathcal{M}_\mu = -1$ pertains to the triplet for which $\delta_\mu = \pi/2$. A value of $\mathcal{M}_\mu = 0$ occurs for a fragment μ with equal weight of the singlet and triplet components. For a spin-pure product, either singlet or triplet, $f\,\mathcal{M} = 1$ holds, since all geminals being singlet imply $\mathcal{M} = f = 1$, and all-but-one geminals singlet and one triplet means $\mathcal{M} = -1 = f$.

Taking the case of a singlet ${}^1\psi_{\mu,0}$ (i.e., $\mathcal{M}_\mu = 1$), the effect of $\hat{H}_\mu$ of Eq.(27) on a singlet

geminal, ${}^1\psi_{\mu,j}$ is

$$\left({}^{\mathcal{N}}\hat{H}_\mu\left(1+\frac{\hat{\mathcal{P}}_{\mu,\mathrm{sf}}}{\mathcal{M}_\mu}\right)-E_{\mu,0}\,\frac{\hat{\mathcal{P}}_{\mu,\mathrm{sf}}}{\mathcal{M}_\mu}\right)|{}^1\psi_{\mu,j}\rangle = (1+1)\,{}^{\mathcal{N}}\hat{H}_\mu|{}^1\psi_{\mu,j}\rangle \;-\; E_{\mu,0}|{}^1\psi_{\mu,j}\rangle$$
$$= (2E_{\mu,j}-E_{\mu,0})|{}^1\psi_{\mu,j}\rangle\ . \tag{A.4}$$

The above result is obviously according to expectations for $j=0$ (belonging to space O_μ) but not for $j\neq 0$.

Staying with $\mathcal{M}_\mu=1$, $\hat{H}_\mu$ of Eq.(27) acting on a triplet $M_S=0$ geminal ${}^3_0\psi_\mu$ results, taking into account Eq.(A.2b)

$$\left({}^{\mathcal{N}}\hat{H}_\mu\left(1+\frac{\hat{\mathcal{P}}_{\mu,\mathrm{sf}}}{\mathcal{M}_\mu}\right)-E_{\mu,0}\,\frac{\hat{\mathcal{P}}_{\mu,\mathrm{sf}}}{\mathcal{M}_\mu}\right)|{}^3_0\psi_\mu\rangle = (1-1)\,{}^{\mathcal{N}}\hat{H}_\mu|{}^3_0\psi_\mu\rangle \;+\; E_{\mu,0}|{}^3_0\psi_\mu\rangle$$
$$= E_{\mu,0}|{}^3_0\psi_\mu\rangle\ . \tag{A.5}$$

Degeneracy of the triplet excited state with the singlet ground state geminal, as reflected by the above can not be reasoned out with their noninteracting character. On one hand, the spin-pure situation is just a limiting case in our approach. Quasi-degeneracy that can be envisaged based on Eq.(A.5) for slight spin-contamination is not welcome. On the other hand, geminals constitute fragments of the many-electron state. Even in the spin-pure limit, the product of two excited triplet geminals has a singlet component and therefore may contribute a divergent term to the PT correction of a singlet ground state if relying on Eq.(A.5).

For a triplet geminal entering the product function $|\mathrm{SLG}\rangle$ from subspace μ, we have $\mathcal{M}_\mu=-1$ and thus $\hat{H}_\mu$ of Eq.(27) acting on a singlet excited geminal ${}^1\psi_{\mu,j}$ results, taking into account Eq.(A.2a)

$$\left({}^{\mathcal{N}}\hat{H}_\mu\left(1+\frac{\hat{\mathcal{P}}_{\mu,\mathrm{sf}}}{\mathcal{M}_\mu}\right)-E_{\mu,0}\,\frac{\hat{\mathcal{P}}_{\mu,\mathrm{sf}}}{\mathcal{M}_\mu}\right)|{}^1\psi_{\mu,j}\rangle = (1-1)\,{}^{\mathcal{N}}\hat{H}_\mu|{}^1\psi_{\mu,j}\rangle \;+\; E_{\mu,0}|{}^1\psi_{\mu,j}\rangle$$
$$= E_{\mu,0}|{}^1\psi_{\mu,j}\rangle\ . \tag{A.6}$$

The case being analogous to that of Eq.(A.5), comments of the previous paragraph apply.

A.3 Hermiticity of Eq.(12)

Examining Hermiticity of $\hat{H}_\mu$ of Eq.(12) one can see that it holds when acting on $M_S = 0$ two-electron functions in subspace μ, but it is spoiled when stepping to $M_S \neq 0$ two-electron states or subspace μ occupied by one or three electrons. Of the terms constituting $\hat{H}_\mu^{\mathrm{eff}}$ of Eq.(12), ${}^{\mathcal{N}}\hat{H}_\mu$ is Hermitian, as both ${}^{\mathcal{N}}\boldsymbol{F}^a$ and ${}^{\mathcal{N}}\boldsymbol{F}^b$ are Hermitian matrices. Making use of $\left({}^{\mathcal{M}}\boldsymbol{F}^a\right)^\dagger = {}^{\mathcal{M}}\boldsymbol{F}^b$ it is easy to see that ${}^{\mathcal{M}}\hat{H}_\mu\,\hat{\mathcal{P}}_{\mu,\mathrm{sf}}$ is self-adjoint in the space spanned by $M_S = 0$ two-electron states, but neither ${}^{\mathcal{M}}\hat{H}_\mu$ nor ${}^{\mathcal{M}}\hat{H}_\mu\,\hat{\mathcal{P}}_{\mu,\mathrm{sf}}$ are self-adjoint in general. To ensure Hermiticity, when term ${}^{\mathcal{M}}\hat{H}_\mu\,\hat{\mathcal{P}}_{\mu,\mathrm{sf}}$ of Eq.(12) is taken into account in defining the zero-order Hamiltonian, it is substituted by its Hermitian part,

$$\left({}^{\mathcal{M}}\hat{H}_\mu\,\hat{\mathcal{P}}_{\mu,\mathrm{sf}}\right)^s = \frac{1}{2}\left({}^{\mathcal{M}}\hat{H}_\mu\,\hat{\mathcal{P}}_{\mu,\mathrm{sf}} + \hat{\mathcal{P}}_{\mu,\mathrm{sf}}\left({}^{\mathcal{M}}\hat{H}_\mu\right)^\dagger\right) \ .$$

This obviously does not introduce any change in the $M_S = 0$ two-electron subspace.

A.4 Spin-pure limit of partitioning variants

We now investigate the effective Hamiltonians formulated in Sec. 2.3.1. Evaluating the effect of either $\hat{H}_\mu^{\mathrm{b}}$ or $\hat{H}_\mu^{\mathrm{c}}$ in the spin-pure case for $\mathcal{M}_\mu = -1$ requires the examination of a limit, since the numerator and the denominator are zero in both cases. A workaround is offered by considering e.g. $\hat{H}_\mu^{\mathrm{c}}$ as

$$\hat{H}_\mu^{\mathrm{c}} = \lim_{\lambda\to 1} \frac{{}^{\mathcal{N}}\hat{H}_\mu + f\,\lambda\,{}^{\mathcal{M}}\hat{H}_\mu^{\mathrm{s}}}{1 + f\,\lambda\,\mathcal{M}/\mathcal{M}_\mu} \ . \tag{A.7}$$

In the spin-pure case with an $M_S = 0$ triplet $\psi_{\mu,0}$, the numerator of the above expression becomes ${}^{\mathcal{N}}\hat{H}_\mu(1-\lambda)$, while the denominator simplifies to $1-\lambda$, allowing the limit to be evaluated as ${}^{\mathcal{N}}\hat{H}_\mu$. The case of $\hat{H}_\mu^{\mathrm{b}}$ is analogous, the effect of the last two terms of the numerator of Eq.(34) on an excited singlet geminal cancel.

As mentioned in Sec. 2.3.1, operator $\hat{H}^{\mathrm{e}}_{\mu}$ as given in Eq.(37) is ill-defined in the spin-pure situation. The limiting case can still be evaluated by inserting λ to the terms containing $\hat{\mathcal{P}}_{\mu,\mathrm{sf}}$ in Eq.(37) and considering the $\lambda \to 1$. Utilizing that $[{}^{\mathcal{N}}\hat{H}_{\mu}, \hat{\mathcal{P}}_{\mu,\mathrm{sf}}] = 0$ holds in space R_{μ} one gets

$$\begin{aligned}\hat{H}^{\mathrm{e}}_{\mu}(\lambda) &= \left(1 + \lambda\,\kappa\,f\,\frac{\mathcal{M}}{\mathcal{M}_{\mu}}\hat{\mathcal{P}}_{\mu,\mathrm{sf}}\right)^{-1}\left({}^{\mathcal{N}}\hat{H}_{\mu} + \lambda\,f\,{}^{\mathcal{M}}\hat{H}_{\mu}\hat{\mathcal{P}}_{\mu,\mathrm{sf}}\right)\\ &= \left(1 + \lambda\,\kappa\,f\,\frac{\mathcal{M}}{\mathcal{M}_{\mu}}\hat{\mathcal{P}}_{\mu,\mathrm{sf}}\right)^{-1}\left(1 + \lambda\,f\,\frac{\mathcal{M}}{\mathcal{M}_{\mu}}\hat{\mathcal{P}}_{\mu,\mathrm{sf}}\right){}^{\mathcal{N}}\hat{H}_{\mu}\ .\end{aligned}$$

Recognizing that $\kappa = 1$ in the spin-pure case results ${}^{\mathcal{N}}\hat{H}_{\mu}$ on the right hand side of the above expression.

B Equivalent energies by different references

If the SLG wavefunction given in Eq.(2) corresponds to the minimum on the HP surface, then

$$|\widetilde{\mathrm{SLG}}\rangle := \hat{\mathcal{P}}_{\mathrm{sf}}|\mathrm{SLG}\rangle = \prod_{\mu=1}^{N/2}\widetilde{\psi}^{+}_{\mu}|\mathrm{vac}\rangle \tag{B.8}$$

yields the same half-projected energy. Quantities corresponding to $|\widetilde{\mathrm{SLG}}\rangle$ will be indicated by a tilde. Based on the expressions given in Ref.[24] the following relationships can be set between quantities corresponding to $|\mathrm{SLG}\rangle$ and $|\widetilde{\mathrm{SLG}}\rangle$. Components of the unnormalized 1-RDM of $|\widetilde{\mathrm{SLG}}\rangle$ read as

$$\begin{aligned}{}^{\mathcal{N}}\widetilde{\boldsymbol{\gamma}}^{a} &= {}^{\mathcal{N}}\boldsymbol{\gamma}^{b}\\ {}^{\mathcal{N}}\widetilde{\boldsymbol{\gamma}}^{b} &= {}^{\mathcal{N}}\boldsymbol{\gamma}^{a}\\ {}^{\mathcal{M}}\widetilde{\boldsymbol{\gamma}}^{a} &= {}^{\mathcal{M}}\boldsymbol{\gamma}^{b}\\ {}^{\mathcal{M}}\widetilde{\boldsymbol{\gamma}}^{b} &= {}^{\mathcal{M}}\boldsymbol{\gamma}^{a}\ .\end{aligned} \tag{B.9}$$

Consequently, Fockians can be evaluated as

$$
\begin{aligned}
{}^{\mathcal{N}}\widetilde{\boldsymbol{F}}^{a} &= {}^{\mathcal{N}}\boldsymbol{F}^{b} \\
{}^{\mathcal{N}}\widetilde{\boldsymbol{F}}^{b} &= {}^{\mathcal{N}}\boldsymbol{F}^{a} \\
{}^{\mathcal{M}}\widetilde{\boldsymbol{F}}^{a} &= {}^{\mathcal{M}}\boldsymbol{F}^{b} \\
{}^{\mathcal{M}}\widetilde{\boldsymbol{F}}^{b} &= {}^{\mathcal{M}}\boldsymbol{F}^{a},
\end{aligned}
\tag{B.10}
$$

while energy-like quantities will be identical to those by $|\mathrm{SLG}\rangle$:

$$
\begin{aligned}
{}^{\mathcal{N}}\widetilde{\Lambda}_{\mu} &= {}^{\mathcal{N}}\Lambda_{\mu} \\
{}^{\mathcal{M}}\widetilde{\Lambda}_{\mu} &= {}^{\mathcal{M}}\Lambda_{\mu} \\
\widetilde{\Theta} &= \Theta \\
\widetilde{E}_{\mu} &= E_{\mu}
\end{aligned}
\tag{B.11}
$$

Using the notation of Sec. 2.3.1, components of the geminal Hamiltonian corresponding to $\widetilde{\psi}_{\mu}$ can be expressed as

$$
\begin{aligned}
{}^{\mathcal{N}}\hat{\widetilde{H}}_{\mu} &= \sum_{kl}^{(\mu)} \left({}^{\mathcal{N}}\boldsymbol{F}^{b}_{kl} k^{+}_{\alpha} l^{-}_{\alpha} \;+\; {}^{\mathcal{N}}\boldsymbol{F}^{a}_{kl} k^{+}_{\beta} l^{-}_{\beta} \right) + \frac{1}{2} \sum_{klmn}^{(\mu)} [kl|mn] \sum_{\sigma,\sigma'} k^{+}_{\sigma} l^{+}_{\sigma'} n^{-}_{\sigma'} m^{-}_{\sigma} \\
{}^{\mathcal{M}}\hat{\widetilde{H}}_{\mu} &= \frac{\mathcal{M}}{\mathcal{M}_{\mu}} \left\{ \sum_{kl}^{(\mu)} \left({}^{\mathcal{M}}\boldsymbol{F}^{b}_{kl} k^{+}_{\alpha} l^{-}_{\alpha} \;+\; {}^{\mathcal{M}}\boldsymbol{F}^{a}_{kl} k^{+}_{\beta} l^{-}_{\beta} \right) + \frac{1}{2} \sum_{klmn}^{(\mu)} [kl|mn] \sum_{\sigma,\sigma'} k^{+}_{\sigma} l^{+}_{\sigma'} n^{-}_{\sigma'} m^{-}_{\sigma} \right\} \\
\widetilde{L}_{\mu} &= L_{\mu}
\end{aligned}
\tag{B.12}
$$

Suppose the unprojected reference used in the PT scheme is $|\widetilde{\mathrm{SLG}}\rangle$. Then the first order interacting space is spanned by the states $\{\widetilde{\Psi}^{(0)}_{K}\}$ $(K \neq 0)$, where $\widetilde{\Psi}^{(0)}_{K}$ is the spin-flip counterpart of $\Psi^{(0)}_{K}$ belonging to the first order interacting space of $|\mathrm{SLG}\rangle$, i.e., $\widetilde{\Psi}^{(0)}_{K} = \hat{\mathcal{P}}_{\mathrm{sf}} \Psi^{(0)}_{K}$. The projected second order energy thus becomes

$$
\widetilde{\mathcal{E}}^{(2)} = \frac{\sum_{K\neq 0} \widetilde{c}^{(1)}_{K} \left(\langle \widetilde{\mathrm{SLG}} | \hat{H} | \widetilde{\Psi}^{(0)}_{K} \rangle + f \, \langle \widetilde{\mathrm{SLG}} | \hat{H} \hat{\mathcal{P}}_{\mathrm{sf}} \widetilde{\Psi}^{(0)}_{K} \rangle - f \, E_{\mathrm{HP}} \langle \widetilde{\mathrm{SLG}} | \hat{\mathcal{P}}_{\mathrm{sf}} \widetilde{\Psi}^{(0)}_{K} \rangle \right)}{1 + f \, \mathcal{M}} \; . \tag{B.13}
$$

Relying on the fact that $[\hat{H}, \hat{\mathcal{P}}_{\rm sf}] = 0$ and $\hat{\mathcal{P}}_{\rm sf}^2 = 1$, it follows that

$$\langle \widetilde{\rm SLG} | \hat{H} | \widetilde{\Psi}_K^{(0)} \rangle = \langle {\rm SLG} | \hat{H} \Psi_K^{(0)} \rangle = H_{0K} \ , \tag{B.14}$$

while

$$\langle \widetilde{\rm SLG} | \hat{H} \hat{\mathcal{P}}_{\rm sf} | \widetilde{\Psi}_K^{(0)} \rangle = \langle {\rm SLG} | \hat{H} \hat{\mathcal{P}}_{\rm sf} | \Psi_K^{(0)} \rangle = \widetilde{H}_{0K} \ . \tag{B.15}$$

Also,

$$\langle \widetilde{\rm SLG} | \hat{\mathcal{P}}_{\rm sf} \widetilde{\Psi}_K^{(0)} \rangle = \langle {\rm SLG} | \hat{\mathcal{P}}_{\rm sf} \Psi_K^{(0)} \rangle = M_{0K} \ . \tag{B.16}$$

Thus

$$\widetilde{\mathcal{E}}^{(2)} = \frac{\sum_{K \neq 0} \widetilde{c}_K^{(1)} (H_{0K} + f \, \widetilde{H}_{0K} - f \, E_{\rm HP} M_{0K})}{1 + f \, \mathcal{M}} \ . \tag{B.17}$$

Coefficients $\widetilde{c}_K^{(1)}$ are obtained as the solution of the system of linear equations

$$\sum_{K \neq 0} \widetilde{G}_{LK} \widetilde{c}_K^{(1)} = - \langle \widetilde{\Psi}_L^{(0)} | \hat{H} | \widetilde{\rm SLG} \rangle \ , \qquad \forall \, L \neq 0 \ . \tag{B.18}$$

Based on Eq.(B.14), the right hand side of Eq.(B.18) is simply $-H_{L0}$, i.e., the same as that of Eq.(18), while coefficient matrix $\widetilde{\boldsymbol{G}}$ is defined as

$$\widetilde{G}_{LK} = \ \langle \widetilde{\Psi}_L^{(0)} | \hat{\widetilde{H}}^{(0)} | \widetilde{\Psi}_K^{(0)} \rangle - \widetilde{E}_0 \delta_{KL} \ . \tag{B.19}$$

Excited states can be given in a concise form as $\widetilde{\Psi}_K^{(0)} = \prod_{\mu=1}^{N/2+1} \widetilde{\varphi}_{\mu,K}^{+} |{\rm vac}\rangle$, where 'creation operator' corresponding to an empty geminal is just the identity. Zero order operator is expressed as a sum of geminal Hamiltonians as

$$\hat{\widetilde{H}}^{(0)} = \sum_{\mu=1}^{N/2+1} \hat{\widetilde{H}}_\mu \ , \tag{B.20}$$

where $\hat{\widetilde{H}}_\mu$ is the analogue of Eq.(28) with $\hat{\widetilde{H}}_\mu \widetilde{\psi}_{\mu,0} = \widetilde{E}_{\mu,0}\widetilde{\psi}_{\mu,0}$. Therefore $\widetilde{E}_0 = \sum_{\mu=1}^{N/2} \widetilde{E}_{\mu,0}$, while

$$\begin{aligned}
\widetilde{G}_{LK} &= \sum_{\mu=1}^{N/2+1} \langle \widetilde{\Psi}_L^{(0)} | \hat{\widetilde{H}}_\mu - \widetilde{E}_{\mu,0} | \widetilde{\Psi}_K^{(0)} \rangle \\
&= \sum_{\mu=1}^{N/2+1} \left\{ \prod_{\nu\neq\mu} \langle \widetilde{\varphi}_{\nu,L} | \widetilde{\varphi}_{\nu,K} \rangle \cdot \langle \widetilde{\varphi}_{\mu,L} | \hat{\widetilde{H}}_\mu - \widetilde{E}_{\mu,0} | \widetilde{\varphi}_{\mu,K} \rangle \right\} \\
&= \sum_{\mu=1}^{N/2+1} \left\{ \prod_{\nu\neq\mu} \langle \varphi_{\nu,L} | \varphi_{\nu,K} \rangle \cdot \langle \widetilde{\varphi}_{\mu,L} | \hat{\widetilde{H}}_\mu - \widetilde{E}'_{\mu,0} | \widetilde{\varphi}_{\mu,K} \rangle \right\} \ .
\end{aligned} \tag{B.21}$$

For comparison,

$$G_{LK} = \sum_{\mu=1}^{N/2+1} \left\{ \prod_{\nu\neq\mu} \langle \varphi_{\nu,L} | \varphi_{\nu,K} \rangle \cdot \langle \varphi_{\mu,L} | \hat{H}_\mu - E_{\mu,0} | \varphi_{\mu,K} \rangle \right\} \ . \tag{B.22}$$

It remains to be shown that with any choice of the partitioning, e.g., any choice of $\hat{\widetilde{H}}_\mu$, zero-order geminal energies fall back to those obtained if SLG is used as a reference. In particular, we need to show that

$$\widetilde{E}_{\mu,0} = \widetilde{E}_{\mu,0} \ , \tag{B.23}$$

and

$$\langle \widetilde{\varphi}_{\mu,L} | \hat{\widetilde{H}}_\mu | \widetilde{\varphi}_{\mu,K} \rangle = \langle \varphi_{\mu,L} | \hat{H}_\mu | \varphi_{\mu,K} \rangle \ . \tag{B.24}$$

Note, that in this case $\widetilde{\varphi}_{\mu,L}$ and $\varphi_{\mu,L}$ are spin-flip counterparts of each other: $\widetilde{\varphi}_{\mu,L} = \hat{\mathcal{P}}_{\rm sf}\varphi_{\mu,L}$, where $\hat{\mathcal{P}}_{\rm sf}$ is understood in the sense of flipping the spin of *all* electrons.

It is straightforward to check that

$$\hat{\mathcal{P}}_{\rm sf}{}^{\mathcal{N}}\hat{\widetilde{H}}_\mu = {}^{\mathcal{N}}\hat{H}_\mu \hat{\mathcal{P}}_{\rm sf} \ , \tag{B.25}$$

and therefore

$$\langle\widetilde{\varphi}_{\mu,L}|^{\mathcal{N}}\hat{\widetilde{H}}_{\mu}|\widetilde{\varphi}_{\mu,K}\rangle = \langle\hat{\mathcal{P}}_{\rm sf}\varphi_{\mu,L}|^{\mathcal{N}}\hat{\widetilde{H}}_{\mu}|\hat{\mathcal{P}}_{\rm sf}\varphi_{\mu,K}\rangle = \langle\varphi_{\mu,L}|^{\mathcal{N}}\hat{H}_{\mu}\hat{\mathcal{P}}^2_{\rm sf}|\varphi_{\mu,K}\rangle = \langle\varphi_{\mu,L}|^{\mathcal{N}}\hat{H}_{\mu}|\varphi_{\mu,K}\rangle \ , \tag{B.26}$$

where $\left(\hat{\mathcal{P}}_{\rm sf}\right)^{\dagger} = \hat{\mathcal{P}}_{\rm sf}$ was taken advantage of. Similarly, utilizing $\hat{\mathcal{P}}_{\rm sf}\,{}^{\mathcal{M}}\hat{\widetilde{H}}_{\mu} = {}^{\mathcal{M}}\hat{H}_{\mu}\,\hat{\mathcal{P}}_{\rm sf}$ combined with the fact that $[\hat{\mathcal{P}}_{\rm sf},\hat{\mathcal{P}}_{\mu,\rm sf}] = 0$ (whether $\hat{\mathcal{P}}_{\mu,\rm sf}$ is understood as local spin-flip or in the sense of Eq.(A.1)) it can be shown that

$$\langle\widetilde{\varphi}_{\mu,L}|^{\mathcal{M}}\hat{\widetilde{H}}_{\mu}\hat{\mathcal{P}}_{\mu,\rm sf} = \langle\varphi_{\mu,L}|^{\mathcal{M}}\hat{H}_{\mu}\hat{\mathcal{P}}_{\mu,\rm sf}|\varphi_{\mu,K}\rangle \tag{B.27}$$

Thus whichever variant of $\hat{H}_{\mu}$ is used, $\langle\widetilde{\varphi}_{\mu,L}|\hat{\widetilde{H}}_{\mu} - \widetilde{E}_{\mu,0}|\widetilde{\varphi}_{\mu,K}\rangle = \langle\varphi_{\mu,L}|\hat{H}_{\mu} - E_{\mu,0}|\varphi_{\mu,K}\rangle$ proving that $\widetilde{\boldsymbol{G}} = \boldsymbol{G}$. That is, the left hand side of Eq.(B.18) coincides with that of Eq.(18), consequently, their solutions are the same: $\widetilde{c}^{(1)}_K = c^{(1)}_K$ ($\forall K \neq 0$). Substituting this result into Eq.(B.17), we arrive at

$$\widetilde{\mathcal{E}}^{(2)} = \frac{\sum_{K\neq 0} c^{(1)}_K (H_{0K} + f\,\widetilde{H}_{0K} - f\,E_{\rm HP}\widetilde{M}_{0K})}{1 + f\,\mathcal{M}} = \mathcal{E}^{(2)} \ . \tag{B.28}$$

C Matrix elements involved in the second order energy expression

This work adopts the notation of Ref.[74] regarding the $M_S = 0$ excitation cases $|\Psi^{(0)}_K\rangle$ belonging to the first order interacting space. To follow the structure more closely, we list matrix elements $\widetilde{H}_{K0} = \langle\Psi^{(0)}_K|\hat{H}\hat{\mathcal{P}}|{\rm SLG}\rangle$ and $M_{K0} = \langle\Psi^{(0)}_K|\hat{\mathcal{P}}_{\rm sf}{\rm SLG}\rangle$ below. Quantities used in Eq.(24) are obtained as $\widetilde{H}_{0K} = \widetilde{H}^*_{K0}$ and $M_{0K} = M^*_{K0}$. For the ξth excited $M_S = 0$ two-electron fragment in subspace μ we use the notation $\psi_{\mu,\xi} = \sum^{(\mu)}_{ij} C_{\substack{ij\\ \xi_\mu}}\, i^+_\beta\, j^+_\alpha|{\rm vac}\rangle$. For convenience, the following notations are used: $\mathcal{M}_{\xi_\mu 0} = \sum\limits_{ij}^{(\mu)} C^*_{\substack{ij\\ \xi_\mu}} C_{ji}$, which is not necessarily zero.

Furthermore,

$$
\begin{aligned}
{}^{M}\gamma^{a}_{\substack{ij\\ \xi_\mu 0}} &:= \frac{\mathcal{M}}{\mathcal{M}_{\mu_i}}\ \langle\psi_{\mu,\xi}|j^+_\alpha i^-_\alpha|\tilde{\psi}_{\mu,0}\rangle = \frac{\mathcal{M}}{\mathcal{M}_{\mu_i}}\ \sum_k^{(\mu)} C^*_{\substack{kj\\ \xi_\mu}} C_{ik} \\
{}^{M}\gamma^{b}_{\substack{ij\\ \xi_\mu 0}} &:= \frac{\mathcal{M}}{\mathcal{M}_{\mu_i}}\ \langle\psi_{\mu,\xi}|j^+_\beta i^-_\beta|\tilde{\psi}_{\mu,0}\rangle = \frac{\mathcal{M}}{\mathcal{M}_{\mu_i}}\ \sum_k^{(\mu)} C^*_{\substack{jk\\ \xi_\mu}} C_{ki} \\
{}^{\mathcal{M}}F^s_{jk} &:= h_{jk} + \frac{1}{\mathcal{M}} \sum_{\tau\neq\mu_j,\mu_k} \sum_{lm}^{\tau} \left({}^{M}\gamma_{lm}[jm|kl] - {}^{M}\gamma^s_{lm}[jm|lk]\right), \quad s\in\{a,b\}\ .
\end{aligned}
\tag{C.29}
$$

Operator $\hat{P}(ij)$ acts on a quantity involving indices i,j as $\hat{P}(ij)z(i,j) = z(i,j) - z(j,i)$.

Matrix element M_{K0} is potentially nonzero only for Case 5 of excitation category II:

1. Category II

   a) Case 5: $\Psi^{(0)}_K = \left(\sum_{ij}^{\mu} C_{\substack{ij\\ \xi_\mu}}\, i^+_\beta j^+_\alpha\right)\left(\sum_{kl}^{\nu} C_{\substack{kl\\ \xi_\nu}}\, k^+_\beta l^+_\alpha\right) \prod_{\rho\neq\mu,\nu} \psi^+_{\rho,0}|\text{vac}\rangle$

$$
M_{K0} = \frac{\mathcal{M}\,\mathcal{M}_{\xi_\mu 0}\,\mathcal{M}_{\xi_\nu 0}}{\mathcal{M}_\mu\,\mathcal{M}_\nu}
\tag{C.30}
$$

Hamiltonian matrix elements are

1. Category II

   a) Case 1: $\Psi^{(0)}_K = i^+_\beta j^+_\alpha k^+_\beta\ l^+_\alpha \prod_{\rho\neq\mu,\nu} \psi^+_{\rho,0}|\text{vac}\rangle\ ,\ i>k, j\in\mu\ ,\ l\in\nu$

$$
\begin{aligned}
\widetilde{H}_{K0} = \frac{\mathcal{M}}{\mathcal{M}_\mu\mathcal{M}_\nu}\ \hat{P}(ik)\Bigg(C_{ji}\left[\sum_{l'}^{\nu} {}^{\mathcal{M}}F^b_{kl'}C_{ll'} + \sum_{l'm'}^{\nu}[kl|m'l']C_{l'm'}\right] \\
+ \sum_{l'}^{\nu} C_{ll'}\left[\sum_{i'}^{\mu}[kj|l'i']C_{i'i} + \sum_{j'}^{\mu}[ik|j'l']C_{jj'}\right]\Bigg)
\end{aligned}
$$

   b) Case 2: $\Psi^{(0)}_K = i^+_\alpha j^+_\beta k^+_\alpha\ l^+_\beta \prod_{\rho\neq\mu,\nu} \psi^+_{\rho,0}|\text{vac}\rangle\ ,\ i>k, j\in\mu\ ,\ l\in\nu$

$$
\begin{aligned}
\widetilde{H}_{K0} = \frac{\mathcal{M}}{\mathcal{M}_\mu\mathcal{M}_\nu}\ \hat{P}(ik)\Bigg(C_{ij}\left[\sum_{l'}^{\nu} {}^{\mathcal{M}}F^a_{kl'}C_{l'l} + \sum_{l'm'}^{\nu}[kl|m'l']C_{m'l'}\right] \\
+ \sum_{l'}^{\nu} C_{l'l}\left[\sum_{i'}^{\mu}[kj|l'i']C_{ii'} + \sum_{j'}^{\mu}[ik|j'l']C_{j'j}\right]\Bigg)
\end{aligned}
$$

c) Case 3: $\Psi_K^{(0)} = i_\alpha^+ j_\alpha^+ \; k_\beta^+ l_\beta^+ \prod_{\rho\neq\mu,\nu} \psi_{\rho,0}^+ |\text{vac}\rangle \ , \ i > j \in \mu \ , \ k > l \in \nu$

$$\widetilde{H}_{K0} = \frac{\mathcal{M}}{\mathcal{M}_\mu \mathcal{M}_\nu} \; \hat{P}(ij)\hat{P}(kl) \sum_{i'}^{\mu} \sum_{k'}^{\nu} C_{ji'} C_{k'l} [ik|k'i']$$

d) Case 5: $\Psi_K^{(0)} = \left(\sum_{ij}^{\mu} C_{\substack{ij \\ \xi_\mu}} i_\beta^+ j_\alpha^+ \right) \left(\sum_{kl}^{\nu} C_{\substack{kl \\ \xi_\nu}} k_\beta^+ l_\alpha^+ \right) \prod_{\rho\neq\mu,\nu} \psi_{\rho,0}^+ |\text{vac}\rangle$

$$\begin{aligned}
\widetilde{H}_{K0} = \frac{\mathcal{M}_{\xi_\mu 0}\mathcal{M}_{\xi_\nu 0}}{\mathcal{M}_\mu \mathcal{M}_\nu} \Big\{ & \sum_{\tau\neq\mu,\nu} \sum_{pq}^{\tau} h_{pq} {}^M\gamma_{qp} + \sum_{\tau\neq\mu,\nu} \frac{\mathcal{M}}{\mathcal{M}_\tau} \sum_{pqrs}^{\tau} C_{pq}^* C_{sr} [pq|rs] \\
& + \frac{1}{2\,\mathcal{M}} \sum_{\substack{\tau,\kappa\neq\mu,\nu \\ \tau\neq\kappa}} \sum_{pr}^{\tau} \sum_{qt}^{\kappa} ({}^M\gamma_{rp} {}^M\gamma_{tq} [pq|rt] - \sum_{s\in\{a,b\}} {}^M\gamma_{rp}^s {}^M\gamma_{tq}^s [pq|tr]) \Big\} \\
& + \frac{\mathcal{M}_{\xi_\mu 0}}{\mathcal{M}_\mu} \Big\{ \sum_{pq}^{\nu} h_{pq} {}^M\gamma_{\substack{qp \\ \xi_\nu 0}} + \frac{1}{\mathcal{M}} \sum_{\tau\neq\mu,\nu} \sum_{pr}^{\nu} \sum_{qt}^{\tau} ({}^M\gamma_{\substack{rp \\ \xi_\nu 0}} {}^M\gamma_{tq} [pq|rt] \\
& \qquad - \sum_{s\in\{a,b\}} {}^M\gamma_{\substack{rp \\ \xi_\nu 0}}^s {}^M\gamma_{tq}^s [pq|tr]) \Big\} \\
& + \frac{\mathcal{M}_{\xi_\nu 0}}{\mathcal{M}_\nu} \Big\{ \sum_{pq}^{\mu} h_{pq} {}^M\gamma_{\substack{qp \\ \xi_\mu 0}} + \frac{1}{\mathcal{M}} \sum_{\tau\neq\mu,\nu} \sum_{pr}^{\mu} \sum_{qt}^{\tau} ({}^M\gamma_{\substack{rp \\ \xi_\mu 0}} {}^M\gamma_{tq} [pq|rt] \\
& \qquad - \sum_{s\in\{a,b\}} {}^M\gamma_{\substack{rp \\ \xi_\mu 0}}^s {}^M\gamma_{tq}^s [pq|tr]) \Big\} \\
& + \frac{\mathcal{M}\mathcal{M}_{\xi_\mu 0}}{\mathcal{M}_\mu \mathcal{M}_\nu} \sum_{cdkl}^{\nu} C_{\substack{kl \\ \xi_\nu}}^* C_{dc} [kl|cd] + \frac{\mathcal{M}\mathcal{M}_{\xi_\nu 0}}{\mathcal{M}_\mu \mathcal{M}_\nu} \sum_{abij}^{\mu} C_{\substack{ij \\ \xi_\mu}}^* C_{ba} [ij|ab] \\
& + \frac{1}{\mathcal{M}} \sum_{ij}^{\mu} \sum_{kl}^{\nu} {}^M\gamma_{\substack{ij \\ \xi_\mu 0}} {}^M\gamma_{\substack{kl \\ \xi_\nu 0}} [jl|ik] - \frac{1}{\mathcal{M}} \sum_{ij}^{\mu} \sum_{kl}^{\nu} \sum_{s\in\{a,b\}} {}^M\gamma_{\substack{ij \\ \xi_\mu 0}}^s {}^M\gamma_{\substack{kl \\ \xi_\nu 0}}^s [jl|ki]
\end{aligned} \tag{C.31}$$

e) Case 16: $\Psi_K^{(0)} = i_\beta^+ j_\alpha^+ k_\beta^+ l_\alpha^+ \prod_{\rho\neq\mu,\nu} \psi_{\rho,0}^+ |\text{vac}\rangle \ , \ i > k \ , \ j > l \in \mu$

$$\widetilde{H}_{K0} = \frac{\mathcal{M}}{\mathcal{M}_\mu \mathcal{M}_\nu} \hat{P}(ik)\hat{P}(jl) C_{lk} \sum_{mn}^{\nu} C_{mn} [ij|nm]$$

2. Category II$\mathcal{V}$

a) Case 1V: $\Psi_K^{(0)} = i_\alpha^+ \; j_\beta^+ \prod_{\rho\neq\mu} \psi_{\rho,0}^+|\text{vac}\rangle \; , \; i \in V \; , \; j \in \mu$

$$\widetilde{H}_{K0} = -\frac{\mathcal{M}}{\mathcal{M}_\mu} \sum_{j'}^{\mu} C_{j'j}{}^{\mathcal{M}} F_{ij'}^a - \frac{\mathcal{M}}{\mathcal{M}_\mu} \sum_{i'j'}^{\mu} C_{i'j'}[ij|i'j']$$

b) Case 2V: $\Psi_K^{(0)} = i_\beta^+ \; j_\alpha^+ \prod_{\rho\neq\mu} \psi_{\rho,0}^+|\text{vac}\rangle \; , \; i \in V \; , \; j \in \mu$

$$\widetilde{H}_{K0} = \frac{\mathcal{M}}{\mathcal{M}_\mu} \sum_{j'}^{\mu} C_{jj'}{}^{\mathcal{M}} F_{ij'}^b + \frac{\mathcal{M}}{\mathcal{M}_\mu} \sum_{i'j'}^{\mu} C_{i'j'}[ij|j'i']$$

c) Case 3V: $\Psi_K^{(0)} = i_\beta^+ \; j_\alpha^+ \prod_{\rho\neq\mu} \psi_{\rho,0}^+|\text{vac}\rangle \; , \; i,j \in V$

$$\widetilde{H}_{K0} = \frac{\mathcal{M}}{\mathcal{M}_\mu} \sum_{kl}^{\mu} C_{lk}[ij|kl]$$

3. Category III

a) Case 8: $\Psi_K^{(0)} = i_\alpha^+ j_\beta^+ k_\alpha^+ l_\beta^+ \; m_\alpha^+ \; n_\beta^+ \prod_{\rho\neq\mu,\nu,\lambda} \psi_{\rho,0}^+|\text{vac}\rangle \; , \; i > k, \; j > l \in \mu \; , \; m \in \nu \; , \; n \in \lambda$

$$\widetilde{H}_{K0} = \frac{\mathcal{M}}{\mathcal{M}_\mu \mathcal{M}_\nu \mathcal{M}_\lambda} \hat{P}(ik)\hat{P}(jl) C_{ij} \sum_{m'}^{\nu} \sum_{n'}^{\lambda} C_{mm'} C_{n'n}[kl|n'm']$$

b) Case 10: $\Psi_K^{(0)} = i_\alpha^+ j_\beta^+ k_\alpha^+ \; l_\beta^+ m_\alpha^+ n_\beta^+ \prod_{\rho\neq\mu,\nu,\lambda} \psi_{\rho,0}^+|\text{vac}\rangle \; , \; i > k, j \in \mu \; , \; l > n, m \in \nu$

$$\widetilde{H}_{K0} = \frac{\mathcal{M}}{\mathcal{M}_\mu \mathcal{M}_\nu \mathcal{M}_\lambda} \hat{P}(ik)\hat{P}(ln) C_{kj} C_{mn} \sum_{op}^{\lambda} C_{po}[il|po]$$

c) Case 12: $\Psi_K^{(0)} = \left(\sum_{ij}^{\mu} C_{\substack{ij \\ \xi_\mu}} i_\beta^+ j_\alpha^+ \right) \; k_\alpha^+ l_\beta^+ m_\alpha^+ \; n_\beta^+ \prod_{\rho\neq\mu,\nu,\lambda} \psi_{\rho,0}^+|\text{vac}\rangle \; , \; k > m, l \in \nu \; , \; n \in \lambda$

$$\widetilde{H}_{K0} = \frac{\mathcal{M}\mathcal{M}_{\xi_\mu 0}}{\mathcal{M}_\mu\mathcal{M}_\nu\mathcal{M}_\lambda}\hat{P}(km)\Big\{C_{kl}\Big[\sum_{n'}^{\lambda} C_{n'n}{}^{\mathcal{M}}F^a_{mn'} + \sum_{n'm'}^{\lambda} C_{m'n'}[mn|m'n']\Big]$$
$$+ \sum_{n'}^{\lambda} C_{n'n}\Big[\sum_{l'}^{\nu} C_{l'l}[km|l'n'] + \sum_{k'}^{\nu} C_{kk'}[ml|n'k']\Big]\Big\}$$
$$+ \hat{P}(km)\frac{C_{kl}}{\mathcal{M}_\nu\mathcal{M}_\lambda}\sum_{n'}^{\lambda} C_{n'n}\sum_{j'j}^{\mu}\Bigg(({}^M\gamma^a_{\substack{j'j\\ \xi_\mu 0}} - \frac{\mathcal{M}_{\xi_\mu 0}}{\mathcal{M}_\mu}{}^M\gamma^a_{j'j})[jm||j'n']$$
$$+({}^M\gamma^b_{\substack{j'j\\ \xi_\mu 0}} - \frac{\mathcal{M}_{\xi_\mu 0}}{\mathcal{M}_\mu}{}^M\gamma^b_{j'j})[jm|j'n']\Bigg) \tag{C.32}$$

d) Case 13: $\Psi^{(0)}_K = \left(\sum_{ij}^{\mu} C_{\substack{ij\\ \xi_\mu}} i^+_\beta j^+_\alpha\right) k^+_\beta l^+_\alpha m^+_\beta\, n^+_\alpha \prod_{\rho\neq\mu,\nu,\lambda} \psi^+_{\rho,0}|\text{vac}\rangle\ ,\ k > m, l \in \nu\ ,\ n \in \lambda$

$$\widetilde{H}_{K0} = \frac{\mathcal{M}\mathcal{M}_{\xi_\mu 0}}{\mathcal{M}_\mu\mathcal{M}_\nu\mathcal{M}_\lambda}\hat{P}(km)\Big\{C_{lk}\Big[\sum_{n'}^{\lambda} C_{nn'}{}^{\mathcal{M}}F^b_{mn'} + \sum_{n'm'}^{\lambda} C_{n'm'}[mn|m'n']\Big]$$
$$+ \sum_{n'}^{\lambda} C_{nn'}\Big[\sum_{l'}^{\nu} C_{ll'}[km|l'n'] + \sum_{k'}^{\nu} C_{k'k}[ml|n'k']\Big]\Big\}$$
$$+ \hat{P}(km)\frac{C_{lk}}{\mathcal{M}_\nu\mathcal{M}_\lambda}\sum_{n'}^{\lambda} C_{nn'}\sum_{j'j}^{\mu}\Bigg(({}^M\gamma^b_{\substack{j'j\\ \xi_\mu 0}} - \frac{\mathcal{M}_{\xi_\mu 0}}{\mathcal{M}_\mu}{}^M\gamma^b_{j'j})[jm||j'n']$$
$$+({}^M\gamma^a_{\substack{j'j\\ \xi_\mu 0}} - \frac{\mathcal{M}_{\xi_\mu 0}}{\mathcal{M}_\mu}{}^M\gamma^a_{j'j})[jm|j'n']\Bigg) \tag{C.33}$$

e) Case 14: $\Psi^{(0)}_K = i^+_\alpha j^+_\alpha\, k^+_\beta l^+_\alpha m^+_\beta\, n^+_\beta \prod_{\rho\neq\mu,\nu,\lambda} \psi^+_{\rho,0}|\text{vac}\rangle\ ,\ i > j \in \mu\ ,\ k > m, l \in \nu\ ,\ n \in \lambda$

$$\widetilde{H}_{K0} = \frac{\mathcal{M}}{\mathcal{M}_\mu\mathcal{M}_\nu\mathcal{M}_\lambda}\hat{P}(ij)\hat{P}(km)C_{lk}\sum_{i'}^{\mu}\sum_{n'}^{\lambda} C_{ii'}C_{n'n}[im|n'i']$$

f) Case 15: $\Psi^{(0)}_K = i^+_\beta j^+_\beta\, k^+_\alpha l^+_\beta m^+_\alpha\, n^+_\alpha \prod_{\rho\neq\mu,\nu,\lambda} \psi^+_{\rho,0}|\text{vac}\rangle\ ,\ i > j \in \mu\ ,\ k > m, l \in \nu\ ,\ n \in \lambda$

$$\widetilde{H}_{K0} = \frac{\mathcal{M}}{\mathcal{M}_\mu\mathcal{M}_\nu\mathcal{M}_\lambda}\hat{P}(ij)\hat{P}(km)C_{kl}\sum_{j'}^{\mu}\sum_{n'}^{\lambda} C_{j'i}C_{nn'}[jm|n'j']$$

4. Category III$\mathcal{V}$

a) Case 4V: $\Psi_K^{(0)} = i_\alpha^+ \; j_\beta^+ k_\alpha^+ l_\beta^+ \prod_{\rho\neq\mu,\nu} \psi_{\rho,0}^+ |\text{vac}\rangle \ , \ i \in V \ , \ j > l, k \in \mu$

$$\widetilde{H}_{K0} = \frac{\mathcal{M}}{\mathcal{M}_\mu \mathcal{M}_\nu} \hat{P}(jl) C_{kl} \sum_{mn}^{\nu} C_{mn} [ij|mn]$$

b) Case 5V: $\Psi_K^{(0)} = i_\beta^+ \; j_\alpha^+ k_\beta^+ l_\alpha^+ \prod_{\rho\neq\mu,\nu} \psi_{\rho,0}^+ |\text{vac}\rangle \ , \ i \in V \ , \ j > l, k \in \mu$

$$\widetilde{H}_{K0} = \frac{\mathcal{M}}{\mathcal{M}_\mu \mathcal{M}_\nu} \hat{P}(jl) C_{lk} \sum_{mn}^{\nu} C_{mn} [ij|nm]$$

c) Case 6V: $\Psi_K^{(0)} = i_\alpha^+ \; j_\beta^+ \; \left(\sum_{kl}^{\nu} C_{\substack{kl \\ \xi_\nu}} k_\beta^+ l_\alpha^+ \right) \prod_{\rho\neq\mu,\nu} \psi_{\rho,0}^+ \; |\text{vac}\rangle \ , \ i \in V \ , \ j \in \mu$

$$\begin{aligned} \widetilde{H}_{K0} = & -\frac{\mathcal{M}\mathcal{M}_{\xi_\nu 0}}{\mathcal{M}_\mu \mathcal{M}_\nu} \Big(\sum_{j'}^{\mu} C_{j'j} {}^{\mathcal{M}}F_{ij'}^a + \sum_{i'j'}^{\mu} C_{i'j'} [ij|i'j'] \Big) \\ & - \frac{1}{\mathcal{M}_\mu} \sum_{j'}^{\mu} C_{j'j} \sum_{kk'}^{\nu} \Bigg(({}^M\gamma_{\substack{k'k \\ \xi_\nu 0}}^a - \frac{\mathcal{M}_{\xi_\nu 0}}{\mathcal{M}_\nu} {}^M\gamma_{k'k}^a)[ik||j'k'] \\ & \qquad + ({}^M\gamma_{\substack{k'k \\ \xi_\nu 0}}^b - \frac{\mathcal{M}_{\xi_\nu 0}}{\mathcal{M}_\nu} {}^M\gamma_{k'k}^b)[ik|j'k'] \Bigg) \end{aligned} \tag{C.34}$$

d) Case 7V: $\Psi_K^{(0)} = i_\beta^+ \; j_\alpha^+ \; \left(\sum_{kl}^{\nu} k_\beta^+ l_\alpha^+ \right) \prod_{\rho\neq\mu,\nu} \psi_{\rho,0}^+ \; |\text{vac}\rangle \ , \ i \in V \ , \ j \in \mu$

$$\begin{aligned} \widetilde{H}_{K0} = & \frac{\mathcal{M}\mathcal{M}_{\xi_\nu 0}}{\mathcal{M}_\mu \mathcal{M}_\nu} \Big(\sum_{j'}^{\mu} C_{jj'} {}^{\mathcal{M}}F_{ij'}^b + \sum_{i'j'}^{\mu} C_{j'i'} [ij|i'j'] \Big) \\ & + \frac{1}{\mathcal{M}_\mu} \sum_{j'}^{\mu} C_{jj'} \sum_{kk'}^{\nu} \Bigg(({}^M\gamma_{\substack{k'k \\ \xi_\nu 0}}^b - \frac{\mathcal{M}_{\xi_\nu 0}}{\mathcal{M}_\nu} {}^M\gamma_{k'k}^b)[ik||j'k'] \\ & \qquad + ({}^M\gamma_{\substack{k'k \\ \xi_\nu 0}}^a - \frac{\mathcal{M}_{\xi_\nu 0}}{\mathcal{M}_\nu} {}^M\gamma_{k'k}^a)[ik|j'k'] \Bigg) \end{aligned} \tag{C.35}$$

e) Case 8V: $\Psi_K^{(0)} = i_\alpha^+ \; j_\alpha^+ \; k_\beta^+ l_\beta^+ \prod_{\rho\neq\mu,\nu} \psi_{\rho,0}^+ \; |\text{vac}\rangle \ , \ i \in V \ , \ j \in \mu \ , \ k > l \in \nu$

$$\widetilde{H}_{K0} = \frac{\mathcal{M}}{\mathcal{M}_\mu \mathcal{M}_\nu} \hat{P}(kl) \sum_{l'}^{\nu} \sum_{j'}^{\mu} C_{l'l} C_{jj'} [ik|l'j']$$

f) Case 9V: $\Psi_K^{(0)} = i_\beta^+ \; j_\beta^+ \; k_\alpha^+ l_\alpha^+ \prod_{\rho\neq\mu,\nu} \psi_{\rho,0}^+ \; |\text{vac}\rangle \ , \ i \in V \ , \ j \in \mu \ , \ k > l \in \nu$

$$\widetilde{H}_{K0} = \frac{\mathcal{M}}{\mathcal{M}_\mu \mathcal{M}_\nu} \hat{P}(kl) \sum_{l'}^{\nu} \sum_{j'}^{\mu} C_{ll'} C_{j'j} [ik|l'j']$$

g) Case 10V: $\Psi_K^{(0)} = i_\alpha^+ j_\alpha^+ \; k_\beta^+ \; l_\beta^+ \prod_{\rho \neq \mu,\nu} \psi_{\rho,0}^+ \; |\text{vac}\rangle \; , \; i > j \in V \; , \; k \in \mu \; , \; l \in \nu$

$$\widetilde{H}_{K0} = \frac{\mathcal{M}}{\mathcal{M}_\mu \mathcal{M}_\nu} \sum_{k'}^{\mu} \sum_{l'}^{\nu} C_{k'k} C_{l'l} [ij||l'k']$$

h) Case 11V: $\Psi_K^{(0)} = i_\beta^+ j_\beta^+ \; k_\alpha^+ \; l_\alpha^+ \prod_{\rho \neq \mu,\nu} \psi_{\rho,0}^+ \; |\text{vac}\rangle \; , \; i > j \in V \; , \; k \in \mu \; , \; l \in \nu$

$$\widetilde{H}_{K0} = \frac{\mathcal{M}}{\mathcal{M}_\mu \mathcal{M}_\nu} \sum_{k'}^{\mu} \sum_{l'}^{\nu} C_{ll'} C_{kk'} [ij||l'k']$$

i) Case 12V: $\Psi_K^{(0)} = i_\beta^+ j_\alpha^+ \; k_\alpha^+ \; l_\beta^+ \prod_{\rho \neq \mu,\nu} \psi_{\rho,0}^+ \; |\text{vac}\rangle \; , \; i, j \in V \; , \; k \in \mu \; , \; l \in \nu$

$$\widetilde{H}_{K0} = \frac{\mathcal{M}}{\mathcal{M}_\mu \mathcal{M}_\nu} \sum_{k'}^{\mu} \sum_{l'}^{\nu} C_{kk'} C_{l'l} [ij|k'l']$$

5. Category IV

a) Case 17: $\Psi_K^{(0)} = i_\alpha^+ j_\beta^+ k_\alpha^+ \; l_\alpha^+ m_\beta^+ n_\alpha^+ \; o_\beta^+ \; p_\beta^+ \prod_{\rho \neq \mu,\nu,\lambda,\sigma} \psi_{\rho,0}^+ |\text{vac}\rangle \; ,$
$i > k, j \in \mu \; , \; l > n, m \in \nu \; , \; o \in \lambda \; , \; p \in \kappa$

$$\widetilde{H}_{K0} = \frac{\mathcal{M}}{\mathcal{M}_\mu \mathcal{M}_\nu \mathcal{M}_\lambda \mathcal{M}_\kappa} \hat{P}(ik) \hat{P}(ln) C_{ij} C_{lm} \sum_{o'}^{\lambda} \sum_{p'}^{\kappa} C_{o'o} C_{p'p} [kn||p'o']$$

b) Case 18: $\Psi_K^{(0)} = i_\beta^+ j_\alpha^+ k_\beta^+ \; l_\beta^+ m_\alpha^+ n_\beta^+ \; o_\alpha^+ \; p_\alpha^+ \prod_{\rho \neq \mu,\nu,\lambda,\kappa} \psi_{\rho,0}^+ |\text{vac}\rangle \; ,$
$i > k, j \in \mu \; , \; l > n, m \in \nu \; , \; o \in \lambda \; , \; p \in \kappa$

$$\widetilde{H}_{K0} = \frac{\mathcal{M}}{\mathcal{M}_\mu \mathcal{M}_\nu \mathcal{M}_\lambda \mathcal{M}_\kappa} \hat{P}(ik) \hat{P}(ln) C_{ji} C_{ml} \sum_{o'}^{\lambda} \sum_{p'}^{\kappa} C_{oo'} C_{pp'} [kn||p'o']$$

c) Case 19: $\Psi_K^{(0)} = i_\alpha^+ j_\beta^+ k_\alpha^+ \; l_\beta^+ m_\alpha^+ n_\beta^+ \; o_\alpha^+ \; p_\beta^+ \prod_{\rho \neq \mu,\nu,\lambda,\kappa} \psi_{\rho,0}^+ |\text{vac}\rangle \; ,$
$i > k, j \in \mu \; , \; l > n, m \in \nu \; , \; o \in \lambda \; , \; p \in \kappa$

$$\widetilde{H}_{K0} = \frac{\mathcal{M}}{\mathcal{M}_\mu \mathcal{M}_\nu \mathcal{M}_\lambda \mathcal{M}_\kappa} \hat{P}(ik)\hat{P}(ln) C_{ij} C_{ml} \sum_{o'}^{\lambda} \sum_{p'}^{\kappa} C_{oo'} C_{p'p} [kn|p'o']$$

6. Category IV$\mathcal{V}$

   a) Case 14V: $\Psi_K^{(0)} = i_\alpha^+ \; j_\alpha^+ k_\beta^+ l_\alpha^+ \; m_\beta^+ \; n_\beta^+ \prod_{\rho \neq \mu,\nu,\lambda} \psi_{\rho,0}^+ \; |\text{vac}\rangle \; ,$
   $i \in V \; , \; j > l, k \in \mu \; , \; m \in \nu \; , \; n \in \lambda$

$$\widetilde{H}_{K0} = \frac{\mathcal{M}}{\mathcal{M}_\mu \mathcal{M}_\nu \mathcal{M}_\lambda} \hat{P}(jl) C_{jk} \sum_{m'}^{\nu} \sum_{n'}^{\lambda} C_{m'm} C_{n'n} [il||m'n']$$

   b) Case 15V: $\Psi_K^{(0)} = i_\beta^+ \; j_\beta^+ k_\alpha^+ l_\beta^+ \; m_\alpha^+ \; n_\alpha^+ \prod_{\rho \neq \mu,\nu,\lambda} \psi_{\rho,0}^+ \; |\text{vac}\rangle \; ,$
   $i \in V \; , \; j > l, k \in \mu \; , \; m \in \nu \; , \; n \in \lambda$

$$\widetilde{H}_{K0} = \frac{\mathcal{M}}{\mathcal{M}_\mu \mathcal{M}_\nu \mathcal{M}_\lambda} \hat{P}(jl) C_{kj} \sum_{m'}^{\nu} \sum_{n'}^{\lambda} C_{mm'} C_{nn'} [il||m'n']$$

   c) Case 16V: $\Psi_K^{(0)} = i_\alpha^+ \; j_\beta^+ k_\alpha^+ l_\beta^+ \; m_\beta^+ \; n_\alpha^+ \prod_{\rho \neq \mu,\nu,\lambda} \psi_{\rho,0}^+ \; |\text{vac}\rangle \; ,$
   $i \in V \; , \; j > l, k \in \mu \; , \; m \in \nu \; , \; n \in \lambda$

$$\widetilde{H}_{K0} = \frac{\mathcal{M}}{\mathcal{M}_\mu \mathcal{M}_\nu \mathcal{M}_\lambda} \hat{P}(jl) C_{kj} \sum_{m'}^{\nu} \sum_{n'}^{\lambda} C_{m'm} C_{nn'} [il|m'n']$$

   d) Case 17V: $\Psi_K^{(0)} = i_\beta^+ \; j_\alpha^+ k_\beta^+ l_\alpha^+ \; m_\beta^+ \; n_\alpha^+ \prod_{\rho \neq \mu,\nu,\lambda} \psi_{\rho,0}^+ \; |\text{vac}\rangle \; ,$
   $i \in V \; , \; j > l, k \in \mu \; , \; m \in \nu \; , \; n \in \lambda$

$$\widetilde{H}_{K0} = \frac{\mathcal{M}}{\mathcal{M}_\mu \mathcal{M}_\nu \mathcal{M}_\lambda} \hat{P}(jl) C_{jk} \sum_{m'}^{\nu} \sum_{n'}^{\lambda} C_{mm'} C_{n'n} [il|m'n']$$

References

(1) Siegbahn, P. E. M.; Almlöf, J.; Heiberg, A.; Roos, B. O. The complete active space SCF (CASSCF) method in a Newton-Raphson formulation with application to the

HNO molecule. *J. Chem. Phys.* **1981**, *74*, 2384–2396.

(2) Vogiatzis, K. D.; Ma, D.; Olsen, J.; Gagliardi, L.; de Jong, W. A. Pushing configuration-interaction to the limit: Towards massively parallel MCSCF calculations. *J. Chem. Phys.* **2017**, *147*, 184111.

(3) Keller, S.; Dolfi, M.; Troyer, M.; Reiher, M. An efficient matrix product operator representation of the quantum chemical Hamiltonian. *J. Chem. Phys.* **2015**, *143*, 244118.

(4) Li Manni, G.; Smart, S. D.; Alavi, A. Combining the Complete Active Space Self-Consistent Field Method and the Full Configuration Interaction Quantum Monte Carlo within a Super-CI Framework, with Application to Challenging Metal-Porphyrins. *J. Chem. Theory Comput.* **2016**, *12*, 1245–1258.

(5) Čížek, J.; Paldus, J. Stability Conditions for the Solutions of the Hartree-Fock Equations for Atomic and Molecular Systems. Application to the Pi-Electron Model of Cyclic Polyenes. *J. Chem. Phys.* **1967**, *47*, 3976–3985.

(6) Yamaguchi, K. The electronic structures of biradicals in the unrestricted Hartree-Fock approximation. *Chem. Phys. Lett.* **1975**, *33*, 330–335.

(7) Jordan, K. D.; Silbey, R. Comments on the use of unrestricted Hartree-Fock theory in orbital energy crossing. *Chem. Phys. Lett.* **1973**, *18*, 27–30.

(8) Pulay, P.; Hamilton, T. P. UHF natural orbitals for defining and starting MC-SCF calculations. *J. Chem. Phys.* **1988**, *88*, 4926–4933.

(9) Bofill, J. M.; Pulay, P. The unrestricted natural orbital-complete active space (UNO-CAS) method: An inexpensive alternative to the complete active space-self-consistent-field (CAS-SCF) method. *J. Chem. Phys.* **1989**, *90*, 3637–3646.

(10) Jiménez-Hoyos, C. A.; Henderson, T. M.; Scuseria, G. E. Generalized Hartree-Fock Description of Molecular Dissociation. *J. Chem. Theory Comput.* **2011**, *7*, 2667–2674.

(11) Scuseria, G. E.; Jiménez-Hoyos, C. A.; Henderson, T. M.; Samanta, K.; Ellis, J. K. Projected quasiparticle theory for molecular electronic structure. *J. Chem. Phys.* **2011**, *135*, 124108.

(12) Li, Z.; Chan, G. K.-L. Spin-Projected Matrix Product States: Versatile Tool for Strongly Correlated Systems. *J. Chem. Theory Comput.* **2017**, *13*, 2681–2695.

(13) Lykos, P.; Pratt, G. W. Discussion on The Hartree-Fock Approximation. *Rev. Mod. Phys.* **1963**, *35*, 496–501.

(14) Nyden, M. R.; Petersson, G. A. Perturbation theory applied to potential energy surfaces. I. The choice of a suitable reference function $\psi(0)$. *J. Chem. Phys.* **1981**, *74*, 6312–6318.

(15) Handy, N. C.; Knowles, P. J.; Somasundram, K. On the convergence of the Møller-Plesset perturbation series. *Theor. Chim. Acta* **1985**, *68*, 87.

(16) Gill, P. M.; Radom, L. Deceptive convergence in Møller-Plesset perturbation energies. *Chem. Phys. Lett.* **1986**, *132*, 16–22.

(17) Jarzęcki, A. A.; Davidson, E. R. Does Unrestricted Møller-Plesset Perturbation Theory for Low Spin Converge When the System Has a Triplet Ground State? *J. Phys. Chem. A* **1998**, *102*, 4742–4746.

(18) Löwdin, P.-O. Quantum Theory of Many-Particle Systems. III. Extension of the Hartree-Fock Scheme to Include Degenerate Systems and Correlation Effects. *Phys. Rev.* **1955**, *97*, 1509–1520.

(19) Löwdin, P.-O. Angular Momentum Wavefunctions Constructed by Projector Operators. *Rev. Mod. Phys.* **1964**, *36*, 966–976.

(20) Jiménez-Hoyos, C. A.; Henderson, T. M.; Tsuchimochi, T.; Scuseria, G. E. Projected Hartree-Fock theory. *J. Chem. Phys.* **2012**, *136*, 164109.

(21) Mayer, I.; Kertész, M. A comparison of different DODS methods when the number of electrons increases. *Int. J. Quantum Chem.* **1976**, *10*, 961–966.

(22) Henderson, T. M.; Scuseria, G. E. Linearized Jastrow-style fluctuations on spin-projected Hartree-Fock. *J. Chem. Phys.* **2013**, *139*, 234113.

(23) Jeszenszki, P.; Surján, P.; Szabados, Á. Spin Symmetry and Size Consistency of Strongly Orthogonal Geminals. *J. Chem. Theor. Comput.* **2015**, *11*, 3096–3103.

(24) Mihálka, Zs. É.; Surján, P. R.; Szabados, Á. Half-Projection of the Strongly Orthogonal Unrestricted Geminals' Product Wave Function. *J. Chem. Theory Comput.* **2020**, *16*, 892–903.

(25) Mayer, I. The Spin-Projected Extended Hartree-Fock Method. In *Adv. Quantum Chem.*; Löwdin, P.-O., Ed.; Academic Press, 1980; Vol. 12; pp 189–262.

(26) Qiu, Y.; Henderson, T. M.; Scuseria, G. E. Communication: Projected Hartree Fock theory as a polynomial similarity transformation theory of single excitations. *J. Chem. Phys.* **2016**, *145*, 111102.

(27) Pons Viver, M. The practical implementation of Löwdin's method for spin projection. *Int. J. Quantum Chem.* **2019**, *119*, e25770.

(28) Amos, A. T.; Hall, G. G. Single determiant wave functions. *Proc. Roy. Soc. (London)* **1961**, *263*, 483–493.

(29) Amos, A. T. Calculations on the ions and lowest π triplet states of some conjugated hydrocarbons. *Mol. Phys.* **1962**, *5*, 91–104.

(30) Schlegel, H. B. Potential energy curves using unrestricted Møller-Plesset perturbation theory with spin annihilation. *J. Chem. Phys.* **1986**, *84*, 4530–4534.

(31) McDouall, J. J. W.; Schlegel, H. B. Analytical gradients for unrestricted Hartree-Fock and second order Møller-Plesset perturbation theory with single spin annihilation. *J. Chem. Phys.* **1989**, *90*, 2363–2369.

(32) Baker, J. Møller-Plesset perturbation theory with the AUHF wavefunction. *Chem. Phys. Lett.* **1988**, *152*, 227–232.

(33) Baker, J. An investigation of the annihilated unrestricted Hartree-Fock wave function and its use in secon-dorder Møller-Plesset perturbation theory. *J. Chem. Phys.* **1989**, *91*, 1789–1795.

(34) Yamaguchi, K.; Takahara, Y.; Fueno, T.; Houk, K. N. Extended Hartree-Fock (EHF) theory of chemical reactions. *Theor. Chim. Acta* **1988**, *73*, 337–364.

(35) Yamanaka, S.; Takeda, R.; Shoji, M.; Kitagawa, Y.; Honda, H.; Yamaguchi, K. Quantum spin correction scheme for ab initio spin-unrestricted solutions: Multiple bonds case. *Int. J. Quantum Chem.* **2005**, *105*, 605–614.

(36) Smeyers, Y. G. Etude d'une fonction unrestricted–Hartree-Fock améliorée. *An. Fis.* **1971**, *67*, 17–24.

(37) Ovchinnikov, A. A.; Labanowski, J. K. Simple spin correction of unrestricted density-functional calculation. *Phys. Rev. A* **1996**, *53*, 3946–3952.

(38) Andrews, J. S.; Jayatilaka, D.; Bone, R. G.; Handy, N. C.; Amos, R. D. Spin contamination in single-determinant wavefunctions. *Chem. Phys. Lett.* **1991**, *183*, 423–431.

(39) Mak, A. M.; Lawler, K. V.; Head-Gordon, M. Approximate spin-projected broken symmetry energies from optimized orbitals that are unrestricted in active pairs. *Chem. Phys. Lett.* **2011**, *515*, 173–178.

(40) Smeyers, Y. G.; Doreste-Suarez, L. Half-Projected and Projected Hartree-Fock Calculations for Singlet Ground States. I. Four-Electron Atomic Systems. *International Journal of Quantum Chemistry* **1973**, *7*, 687–698.

(41) Smeyers, Y. G.; Bruceña, A. M. Half-projected Hartree-Fock model for computing potential-energy surfaces. *Int. J. Quantum Chem.* **1978**, *14*, 641–648.

(42) Ruiz, M. B.; Mayer, I. Deriving gradient formulae for SCF methods by using Brillouin-type theorems. Gradient in the HPHF method. *Chem. Phys. Lett.* **1995**, *236*, 217–228.

(43) Ruiz, M.; Otto, P.; Smeyers, Y. G. The simplex method for geometry optimization in half-projected Hartree-Fock calculations of excited states. *J. Mol. Struct.: THEOCHEM* **1996**, *365*, 151–165.

(44) Cox, P.; Wood, M. H. The half-projected Hartree-Fock method. *Theor. Chim. Acta* **1976**, *41*, 269–278.

(45) Lengsfield, B. H.; Phillips, D. H.; Schug, J. C. Half-projected Hartree-Fock calculations on several small molecules. *J. Chem. Phys.* **1981**, *74*, 5174–5180.

(46) Olivella, S.; Salvador, J. The half-projected Hartree-Fock model for computing thermally "forbidden" pericyclic reactions and biradical processes. I. Formulation and results for some singlet biradical species. *Int. J. Quantum Chem.* **1990**, *37*, 713–728.

(47) Bone, R. G. A.; Pulay, P. Half-projected Hartree-Fock natural orbitals for defining CAS-SCF active spaces. *Int. J. Quantum Chem.* **1993**, *45*, 133–166.

(48) Smeyers, Y. G.; Fernandez-Serra, P.; Ruiz, M. B. An Application of the Half-projected Hartree-Fock Model to the Direct Determination of the Lowest Singlet and Triplet Excited States of Molecular Systems. In *Strategies and Applications in Quantum Chemistry: From Molecular Astrophysics to Molecular Engineering*; Ellinger, Y., Defranceschi, M., Eds.; Kluwer Academic Publishers: Dordrecht, 1996; pp 175–188.

(49) Smeyers, Y. G.; Ruiz, M.; Otto, P. P. The half projected Hartree-Fock function for determining singlet excited states. Application to cyclobutanone and 3-cyclopenten-1-one. *J. Mol. Struct.: THEOCHEM* **1997**, *390*, 91–99.

(50) Otto, P.; Ruiz, M. The multiconfiguration half-projected Hartree-Fock (MCHPHF) method and its application to low-lying singlet excited states of ketene, allene and benzene. *J. Mol. Struct.: THEOCHEM* **1998**, *433*, 131–139.

(51) Ye, H.-Z.; Van Voorhis, T. Half-Projected σ Self-Consistent Field For Electronic Excited States. *J. Chem. Theory Comput.* **2019**, *15*, 2954–2965.

(52) Smeyers, Y. G. The half projected Hartree–Fock model for determining singlet excited states. In *Adv. Quantum. Chem.*; Löwdin, P.-O., Sabin, J. R. S., Zerner, M. C., Brändas, E., Lami, A., Barone, V., Eds.; Academic Press, 2000; Vol. 36; pp 253–270.

(53) Smeyers, Y. G.; Delgado-Barrio, G. Analysis of the half-projected Hartree-Fock function: Density matrix, natural orbitals, and configuration interaction equivalence. *Int. J. Quantum Chem.* **1976**, *10*, 461–472.

(54) Botella, V.; Castaño, O.; Fernández-Serra, P.; Smeyers, Y. Multiple solutions and spatial symmetry properties of singlet and triplet states in the half-projected Hartree-Fock method. *Chem. Phys. Lett.* **1994**, *219*, 497–501.

(55) Arai, T. Theorem on Separability of Electron Pairs. *J. Chem. Phys.* **1960**, *33*, 95–98.

(56) Surján, P. R. *Topics in current chemistry* **1999**, *203*, 63–88.

(57) Bobrowicz, F. W.; Goddard-III, W. A. The Self-Consistent Field Equations for Generalized Valence Bond and Open-Shell Hartree–Fock Wave Functions. In *Methods of Electronic Structure Theory*; Schaefer-III, H. F., Ed.; Plenum: New York, 1977; p 79–127.

(58) Lawler, K. V.; Small, D. W.; Head-Gordon, M. Orbitals That Are Unrestricted in Active Pairs for Generalized Valence Bond Coupled Cluster Methods. *J. Phys. Chem. A* **2010**, *114*, 2930–2938.

(59) Beran, G. J. O.; Austin, B.; Sodt, A.; Head-Gordon, M. Unrestricted Perfect Pairing: The Simplest Wave-Function-Based Model Chemistry beyond Mean Field. *J. Phys. Chem. A* **2005**, *109*, 9183–9192.

(60) Rassolov, V. A. A geminal model chemistry. *J. Chem. Phys.* **2002**, *117*, 5978–5987.

(61) Rassolov, V. A.; Xu, F. Geminal model chemistry III: Partial spin restriction. *J. Chem. Phys.* **2007**, *126*, 234112.

(62) Rassolov, V. A.; Xu, F.; Garashchuk, S. Geminal model chemistry II. Perturbative corrections. *J. Chem. Phys.* **2004**, *120*, 10385–10394.

(63) Rosta, E.; Surján, P. R. Interaction of chemical bonds. V. Perturbative corrections to geminal-type wave functions. *Int. J. Quantum Chem.* **2000**, *80*, 96–104.

(64) Rosta, E.; Surján, P. R. Two-body zeroth order Hamiltonians in multireference perturbation theory: The APSG reference state. *J. Chem. Phys.* **2002**, *116*, 878–890.

(65) Kobayashi, M.; Szabados, Á.; Nakai, H.; Surján, P. R. Generalized Møller-Plesset Partitioning in Multiconfiguration Perturbation Theory *J. Chem. Theory. Comput.* **2010**, *6*, 2024–2033.

(66) Tarumi, M.; Kobayashi, M.; Nakai, H. Generalized Møller–Plesset Multiconfiguration Perturbation Theory Applied to an Open-Shell Antisymmetric Product of Strongly Orthogonal Geminals Reference Wave Function. *J. Chem. Theory Comput.* **2012**, *8*, 4330–4335.

(67) Kutzelnigg, W. Separation of strong (bond-breaking) from weak (dynamical) correlation. *Chem. Phys.* **2012**, *401*, 119–124.

(68) Li, S.; Ma, J.; Jiang, Y. Pair-correlated coupled cluster theory: An alternative multireference coupled cluster method. *J. Chem. Phys.* **2003**, *118*, 5736–5745.

(69) Fang, T.; Li, S. Block correlated coupled cluster theory with a complete active-space self-consistent-field reference function: The formulation and test applications for single bond breaking. *J. Chem. Phys.* **2007**, *127*, 204108.

(70) Zoboki, T.; Szabados, Á.; Surján, P. R. Linearized Coupled Cluster Corrections to Antisymmetrized Product of Strongly Orthogonal Geminals: Role of Dispersive Interactions. *J. Chem. Theory Comput.* **2013**, *9*, 2602–2608.

(71) Margócsy, Á.; Szabados, Á. Ring coupled cluster doubles at the multireference level. *J. Chem. Phys.* **2020**, *152*, 204114.

(72) Chatterjee, K.; Pernal, K. Excitation energies from extended random phase approximation employed with approximate one- and two-electron reduced density matrices. *J. Chem. Phys.* **2012**, *137*, 204109.

(73) Pernal, K. Intergeminal Correction to the Antisymmetrized Product of Strongly Orthogonal Geminals Derived from the Extended Random Phase Approximation. *J. Chem. Theory Comput.* **2014**, *10*, 4332–4341.

(74) Földvári, D.; Tóth, Zs.; Surján, P. R.; Szabados, Á. Geminal perturbation theory based on the unrestricted Hartree-Fock wavefunction. *J. Chem. Phys.* **2019**, *150*, 034103.

(75) Robinson, P. D. H_2^+: A Problem in Perturbation Theory. *Proc. Phys. Soc.* **1961**, *78*, 537–548.

(76) Hirschfelder, J. O.; Silbey, R. New Type of Molecular Perturbation Treatment. *J. Chem. Phys.* **1966**, *45*, 2188–2192.

(77) Hirschfelder, J. O. Perturbation Theory for Exchange Forces. *Chem. Phys. Lett.* **1967**, *1*, 325–329.

(78) Hirschfelder, J. O. Perturbation Theory for Exchange Forces, II. *Chem. Phys. Lett.* **1967**, *1*, 363–368.

(79) Van der Avoird, A. Perturbation Theory for Intermolecular Interactions in the Wave-Operator Formalism. *J. Chem. Phys.* **1967**, *47*, 3649–3653.

(80) Van der Avoird, A. Note on a Perturbation Theory for Intermolecular Interactions in the Wave Operator Formalism. *Chem. Phys. Lett.* **1967**, *1*, 411–412.

(81) Murrell, J. N.; Shaw, G. Intermolecular Forces in the Region of Small Orbital Overlap. *J. Chem. Phys.* **1967**, *46*, 1768–1772.

(82) Claverie, P. Theory of intermolecular forces. I. On the inadequacy of the usual Rayleigh-Schrödinger perturbation method for the treatment of intermolecular forces. *Int. J. Quantum Chem.* **1971**, *5*, 273–296.

(83) Jeziorski, B.; Kołos, W. On Symmetry Forcing in Perturbation Theory of Weak Inter-Molecular Interactions. *Int. J. Quantum Chem. (Suppl. 1)* **1977**, *12*, 91–117.

(84) Chałasiński, G.; Jeziorski, B.; Szalewicz, K. On the convergence properties of the Rayleigh-Schrödinger and the Hirschfelder-Silbey perturbation expansions for molecular interaction energies. *Int. J. Quantum. Chem.* **1977**, *11*, 247–257.

(85) Jeziorski, B.; Szalewicz, K.; Chałasiński, G. Symmetry Forcing and Convergence Properties of Perturbation Expansions for Molecular Interaction Energies. *Int. J. Quantum. Chem.* **1978**, *14*, 271–287.

(86) Jeziorski, B.; Moszynski, R.; Szalewicz, K. Perturbation Theory Approach to Intermolecular Potential Energy Surfaces of van der Waals Complexes. *Chem. Rev.* **1994**, *94*, 1887–1930.

(87) Surján, P. R. Interaction of chemical bonds: Strictly localized wave functions in orthogonal basis. *Phys. Rev. A* **1984**, *30*, 43–50.

(88) Surján, P. R.; Mayer, I.; Lukovits, I. Interaction of chemical bonds. II. Ab initio theory for overlap, delocalization, and dispersion interactions. *Phys. Rev. A* **1985**, *32*, 748–755.

(89) Surján, P. R. The interaction of chemical bonds. III. Perturbed strictly localized geminals in LMO basis. *Int. J. Quantum Chem.* **1994**, *52*, 563–574.

(90) Pople, J.; Binkley, J.; Seeger, R. Theoretical models incorporating electron correlation. *Int. J. Quantum Chem.* **1976**, *10*, 1–19.

(91) Hurley, A. C.; Lennard-Jones, J.; Pople, J. A. The Molecular Orbital Theory of Chemical Valency. XVI. A Theory of Paired-Electrons in Polyatomic Molecules. *Proc. Roy. Soc. (London)* **1953**, *220*, 446–455.

(92) Parks, J. M.; Parr, R. G. Theory of Separated Electron Pairs. *J. Chem. Phys.* **1957**, *28*, 335–345.

(93) Surján, P. Geminal Approach. In *Reference Module in Chemistry, Molecular Sciences and Chemical Engineering*; Elsevier, 2016.

(94) Xu, E.; Li, S. Block correlated second order perturbation theory with a generalized valence bond reference function. *J. Chem. Phys.* **2013**, *139*, 174111.

(95) Kapuy, E. Extension of the separated pair theory. *Theor. Chim. Acta* **1966**, *6*, 281–291.

(96) Kapuy, E. Application of the extended separated pair theory to the π-electrons of trans-butadiene without zero differential overlap approximation. *Theor. Chim. Acta* **1968**, *12*, 397–404.

(97) Tsuchimochi, T.; Ten-no, S. L. Second-Order Perturbation Theory with Spin-Symmetry-Projected Hartree-Fock. *J. Chem. Theory Comput.* **2019**, *15*, 6688–6702.

(98) Tsuchimochi, T.; Va Voorhis, T. Extended Møller-Plesset perturbation theory for dynamical and static correlations. *J. Chem. Phys.* **2014**, *141*, 164117.

(99) Knowles, P. J.; Handy, N. C. Projected unrestricted Møller-Plesset second-order energies. *J. Chem. Phys.* **1988**, *88*, 6991–6998.

(100) Amos, A. T. On the Derivation of Symmetry Adapted Perturbation Theories. *Chem. Phys. Lett.* **1970**, *5*, 587–590.

(101) Peierls, R. Perturbation Theory for Projected States. *Proc. R. Soc. Lond. A* **1973**, *333*, 157–170.

(102) Belén Ruiz, M. A partially projected wave function for radicals. *J. Math. Chem.* **1998**, *24*, 233–248.

(103) Lengsfield, B. H.; Schug, J. C. Approximate spin-extended Hartree-Fock calculations. *Chem. Phys. Lett.* **1978**, *57*, 442–445.

(104) Löwdin, P.-O. Band Theory, Valence Bond, and Tight-Binding Calculations. *J. Appl. Phys.* **1962**, *33*, 251–280, Suppl.

(105) Jeszenszki, P.; Rassolov, V.; Surján, P. R.; Szabados, Á. Local spin from strongly orthogonal geminal wavefunctions. *Mol. Phys.* **2015**, *113*, 249–251.

(106) Huber, K. P.; Herzberg, G. *Molecular Spectra and Molecular Structure— IV. Constants of Diatomic Molecules*; Van Nostrand Reinhold: New York, 1979.

(107) Dunning, T. H. Gaussian basis sets for use in correlated molecular calculations. I. The atoms boron through neon and hydrogen. *J. Chem. Phys.* **1989**, *90*, 1007–1023.

(108) Slipchenko, L. V.; Krylov, A. I. Singlet-triplet gaps in diradicals by the spin-flip approach: A benchmark study. *J. Chem. Phys.* **2002**, *117*, 4694–4708.

(109) Borowski, P.; Fülscher, M.; Malmqvist, P.-Å.; Roos, B. O. A theoretical study of the low-lying excited states of ozone. *Chem. Phys. Lett.* **1995**, *237*, 195–203.

(110) Hay, P. J.; Dunning Jr, T. H. Geometries and energies of the excited states of O_3 from ab initio potential energy surfaces. *J. Chem. Phys.* **1977**, *67*, 2290–2303.

(111) Szalay, P. G.; Bartlett, R. J. Analytic energy gradients for the twoâdeterminant coupled cluster method with application to singlet excited states of butadiene and ozone. *J. Chem. Phys.* **1994**, *101*, 4936–4944.

(112) Musiał, M.; Kucharski, S. A.; Zerzucha, P.; Kuś, T.; Bartlett, R. J. *J. Chem. Phys.* Excited and ionized states of the ozone molecule with full triples coupled cluster methods. **2009**, *131*, 194104.

(113) Jagau, T.-C.; Gauss, J. Linear-response theory for Mukherjee's multireference coupled-cluster method: Excitation energies. *J. Chem. Phys.* **2012**, *137*, 044116.

(114) Woon, D. E.; Dunning Jr., T. H. Gaussian basis sets for use in correlated molecular calculations. V. Core-valence basis sets for boron through neon. *J. Chem. Phys.* **1995**, *103*, 4572–4585.

(115) Thunemann, K.-H.; Peyerimhoff, S. D.; Buenker, R. J. Configuration interaction calculations for the ground and excited states of ozone and its positive ion: Energy locations and transition probabilities. *J. Mol. Spectrosc.* **1978**, *70*, 432–448.

(116) Wenthold, P. G.; Squires, R. R.; Lineberger, W. C. Ultraviolet Photoelectron Spectroscopy of the o-, m-, and p-Benzyne Negative Ions. Electron Affinities and Singlet–Triplet Splittings for o-, m-, and p-Benzyne. *J. Am. Chem. Soc.* **1998**, *120*, 5279–5290.